

# A SYMMETRIZED PARAMETRIC FINITE ELEMENT METHOD FOR ANISOTROPIC SURFACE DIFFUSION IN THREE DIMENSIONS\*

WEIZHU BAO<sup>†</sup> AND YIFEI LI<sup>†</sup>

**Abstract.** We extend the symmetrized parametric finite method for the evolution of a closed curve under anisotropic surface diffusion in two dimensions, recently proposed by us [W. Bao, W. Jiang, and Y. Li, *SIAM J. Numer. Anal.*, 61 (2023), pp. 617–641], to the evolution of a closed and orientable surface under anisotropic surface diffusion with a general anisotropic surface energy  $\gamma(\mathbf{n})$  in three dimensions (3D), where  $\mathbf{n} \in \mathbb{S}^2$  is the unit outward normal vector. By introducing a novel symmetric positive definite surface energy matrix  $Z_k(\mathbf{n})$  depending on a stabilizing function  $k(\mathbf{n}) : \mathbb{S}^2 \rightarrow \mathbb{R}$  and the Cahn–Hoffman  $\xi$ -vector, we present a new symmetrized variational formulation for anisotropic surface diffusion in 3D with weakly or strongly anisotropic surface energy. The variational problem preserves two important structures, volume conservation and energy dissipation. Then we propose a structure-preserving parametric finite element method (SP-PFEM) to discretize the symmetrized variational problem in space via PFEM and in time via an implicit-explicit Euler method, which preserves the volume in the discretized level. Under a relatively mild and simple condition on  $\gamma(\mathbf{n})$ , we show that the SP-PFEM is unconditionally energy stable for almost all anisotropic surface energies  $\gamma(\mathbf{n})$  arising in practical applications. Thus the proposed SP-PFEM preserves the two important structures of the original anisotropic surface diffusion in the discretized level. Extensive numerical results are reported to demonstrate the efficiency and accuracy as well as the structure-preserving properties of the proposed SP-PFEM for solving anisotropic surface diffusion in 3D.

**Key words.** anisotropic surface diffusion, Cahn–Hoffman  $\xi$ -vector, anisotropic surface energy, parametric finite element method, structure-preserving, surface energy matrix, energy-stable

**MSC codes.** 65M60, 65M12, 35K55, 53C44

**DOI.** 10.1137/22M1500575

**1. Introduction.** In materials science and solid-state physics as well as many other applications, surface energy is usually anisotropic due to lattice orientational anisotropy at material interfaces and/or surfaces [43, 27]. The anisotropic surface energy generates *anisotropic surface diffusion*—an important and general process involving the motion of adatoms, molecules, and atomic clusters (adparticles)—at materials surfaces and interfaces in solids [20]. The anisotropic surface diffusion is an important kinetics and/or mechanism in surface phase formation [18, 21], epitaxial growth [26, 28], heterogeneous catalysis [29], and other areas in materials/surface science [44]. It has significant and manifested applications in solid-state physics and materials science as well as computational geometry, such as solid-state dewetting [32, 38, 45, 44, 49], crystal growth of nanomaterials [15], evolution of voids in microelectronic circuits [36, 47], morphology development of alloys [2], quantum dots manufacturing [1], deformation of images [22], etc.

---

\* Submitted to the journal's Methods and Algorithms for Scientific Computing section June 2, 2022; accepted for publication (in revised form) January 23, 2023; published electronically July 5, 2023.

<https://doi.org/10.1137/22M1500575>

**Funding:** The first author's research was supported by the Ministry of Education of Singapore, grant MOE2019-T2-1-063 (R-146-000-296-12).

<sup>†</sup> Department of Mathematics, National University of Singapore, Singapore, 119076 (matbaowz@nus.edu.sg, e0444158@u.nus.edu).

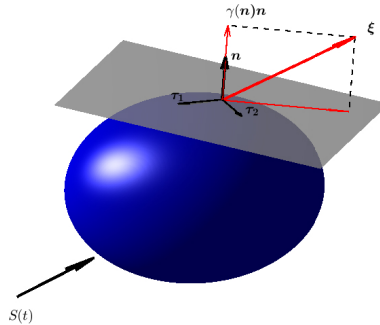


FIG. 1.1. An illustration of a closed and orientable surface  $S := S(t)$  in  $\mathbb{R}^3$  under anisotropic surface diffusion with an anisotropic surface energy  $\gamma(\mathbf{n})$ , where  $\mathbf{n}$  is the outward unit normal vector,  $\xi$  is the Cahn–Hoffman  $\xi$ -vector in (1.3), and  $\tau_1$  and  $\tau_2$  form a basis of the local tangential space.

As shown in Figure 1.1, for a closed and orientable surface  $S := S(t)$  in three dimensions (3D) associated with a given anisotropic surface energy  $\gamma(\mathbf{n})$ , where  $t \geq 0$  is time and  $\mathbf{n} = (n_1, n_2, n_3)^T \in \mathbb{S}^2$  represents the outward unit normal vector satisfying  $|\mathbf{n}| := \sqrt{n_1^2 + n_2^2 + n_3^2} = 1$ . The motion by anisotropic surface diffusion of the surface is described by the following geometric flow [37, 32, 38, 45, 44, 49]:

$$(1.1) \quad V_n = \Delta_S \mu,$$

where  $V_n$  denotes the normal velocity,  $\Delta_S := \nabla_S \cdot \nabla_S$  is the surface Laplace–Beltrami operator,  $\nabla_S$  denotes the surface gradient with respect to the surface  $S(t)$ , and  $\mu := \mu(\mathbf{n}, \nabla_S \mathbf{n})$  is the chemical potential (or weighted mean curvature denoted as  $H_\gamma := H_\gamma(\mathbf{n}, \nabla_S \mathbf{n})$  in the literature) generated from the surface energy functional  $W(S) := W(S(t)) = \int_{S(t)} \gamma(\mathbf{n}) dA$  with  $dA$  representing the surface integral via the thermodynamic variation as  $\mu = \frac{\delta W(S)}{\delta S} = \lim_{\varepsilon \rightarrow 0} \frac{W(S^\varepsilon) - W(S)}{\varepsilon}$  with  $S^\varepsilon$  being a small perturbation of  $S$  [33, 34]. It is well-known that the evolution of the surface  $S(t)$  under the anisotropic surface diffusion (1.1) preserves the following two essential geometric structures [20]: (1) the volume of the region enclosed by the surface is conserved, and (2) the free surface energy (or weighted surface area)  $W(S)$  decreases in time. In fact, the motion governed by the anisotropic surface diffusion can be mathematically regarded as the  $H^{-1}$ -gradient flow of the free surface energy functional (or weighted surface area)  $W(S)$  [41].

Define  $\gamma(\mathbf{p}) : \mathbb{R}^3 \rightarrow \mathbb{R}_{\geq 0}$  to be a homogeneous extension of the anisotropic surface energy  $\gamma(\mathbf{n}) : \mathbb{S}^2 \rightarrow \mathbb{R}^+$  satisfying (i)  $\gamma(c\mathbf{p}) = c\gamma(\mathbf{p})$  for  $c > 0$  and  $\mathbf{p} \in \mathbb{R}^3$ , and (ii)  $\gamma(\mathbf{p})|_{\mathbf{p}=\mathbf{n}} = \gamma(\mathbf{n})$  for  $\mathbf{n} \in \mathbb{S}^2$ . A typical homogeneous extension is widely used in the literature as [34, 24]

$$(1.2) \quad \gamma(\mathbf{p}) := \begin{cases} |\mathbf{p}| \gamma\left(\frac{\mathbf{p}}{|\mathbf{p}|}\right) & \forall \mathbf{p} = (p_1, p_2, p_3)^T \in \mathbb{R}_*^3 := \mathbb{R}^3 \setminus \{\mathbf{0}\}, \\ 0, & \mathbf{p} = \mathbf{0}, \end{cases}$$

where  $|\mathbf{p}| = \sqrt{p_1^2 + p_2^2 + p_3^2}$ . Then the Cahn–Hoffman  $\xi$ -vector introduced by Cahn and Hoffman and the Hessian matrix  $\mathbf{H}_\gamma(\mathbf{n})$  of  $\gamma(\mathbf{p})$  are mathematically given by [31, 46]

$$(1.3) \quad \xi = (\xi_1, \xi_2, \xi_3)^T := \xi(\mathbf{n}) = \nabla \gamma(\mathbf{p})|_{\mathbf{p}=\mathbf{n}}, \quad \mathbf{H}_\gamma(\mathbf{n}) := \nabla \nabla \gamma(\mathbf{p})|_{\mathbf{p}=\mathbf{n}} \quad \forall \mathbf{n} \in \mathbb{S}^2.$$

It is easy to check that  $\xi \cdot \mathbf{n} = \gamma(\mathbf{n})$  for  $\mathbf{n} \in \mathbb{S}^2$  [31, 46]. Then the chemical potential  $\mu$  (or weighted mean curvature  $H_\gamma$ ) can be obtained as [19]

$$(1.4) \quad \mu = \mu(\mathbf{n}, \nabla_S \mathbf{n}) = H_\gamma = H_\gamma(\mathbf{n}, \nabla_S \mathbf{n}) = \nabla_S \cdot \xi = \nabla_S \cdot \xi(\mathbf{n}) \quad \forall \mathbf{n} \in \mathbb{S}^2.$$

For any  $\mathbf{n} \in \mathbb{S}^2$ , we notice that  $\mathbf{H}_\gamma(\mathbf{n})\mathbf{n} = \mathbf{0} \in \mathbb{R}^3$  and thus 0 is an eigenvalue of  $\mathbf{H}_\gamma(\mathbf{n})$  and  $\mathbf{n}$  is a corresponding eigenvector. We denote the other two eigenvalues of  $\mathbf{H}_\gamma(\mathbf{n})$  as  $\lambda_1(\mathbf{n}) \leq \lambda_2(\mathbf{n}) \in \mathbb{R}$ . When  $\gamma(\mathbf{n}) \equiv \text{constant}$  (e.g.,  $\gamma(\mathbf{n}) \equiv 1$ ) for  $\mathbf{n} \in \mathbb{S}^2$ , i.e., with isotropic surface energy, then we have  $\gamma(\mathbf{p}) = |\mathbf{p}|$  in (1.2),  $\xi = \mathbf{n}$  in (1.3), and  $\mu = H$  and  $\mathbf{H}_\gamma(\mathbf{n}) \equiv I_3 - \mathbf{n}\mathbf{n}^T$  in (1.3) with  $H$  the mean curvature and  $I_3$  the  $3 \times 3$  identity matrix, and  $\lambda_1(\mathbf{n}) = \lambda_2(\mathbf{n}) \equiv 1$ , and thus the anisotropic surface diffusion (1.1) collapses to the (isotropic) surface diffusion with normal velocity given as  $V_n = \Delta_S H$  [10, 37]. In contrast, when  $\gamma(\mathbf{n})$  is not a constant, i.e., with anisotropic surface energy, when  $\tau^T \mathbf{H}_\gamma(\mathbf{n}) \tau \geq 0$  for all  $\mathbf{n}, \tau \in \mathbb{S}^2$  satisfying  $\tau \cdot \mathbf{n} := \tau^T \mathbf{n} = 0$  ( $\Leftrightarrow \lambda_2(\mathbf{n}) \geq \lambda_1(\mathbf{n}) \geq 0$  for all  $\mathbf{n} \in \mathbb{S}^2$   $\Leftrightarrow$  the Frank diagram of  $\gamma(\mathbf{n})$  is convex), it is called *weakly anisotropic*, and when  $\tau^T \mathbf{H}_\gamma(\mathbf{n}) \tau$  changes sign for  $\mathbf{n}, \tau \in \mathbb{S}^2$  satisfying  $\tau \cdot \mathbf{n} = 0$  ( $\Leftrightarrow \lambda_1(\mathbf{n}) < 0$  for some  $\mathbf{n} \in \mathbb{S}^2$   $\Leftrightarrow$  the Frank diagram of  $\gamma(\mathbf{n})$  is not convex), it is called *strongly anisotropic*. For the convenience of the readers, we list several commonly used anisotropic surface energies  $\gamma(\mathbf{n})$  in the literature and their corresponding Cahn–Hoffman  $\xi$ -vectors in Appendix A.

Different numerical methods have been presented for solving the isotropic and anisotropic surface diffusion (1.1), such as the finite element method via graph evolution [3, 24, 23, 30], the marker-particle method [25], the discontinuous Galerkin finite element method [48], the parametric method for curve in higher codimension [39], and the parametric finite element method (PFEM) [10, 13, 30, 7, 34, 35, 8]. Among these methods, for isotropic surface diffusion, the energy-stable PFEM (ES-PFEM) based on an elegant variational formulation, which was proposed by Barrett, Garcke, and Nürnberg [10, 12] (denoted the BGN scheme), performs the best in terms of efficiency and accuracy as well as mesh quality in practical computations, especially in two dimensions (2D). The BGN scheme with unconditional energy stability was successfully extended for solving solid-state dewetting problems with isotropic surface energy, i.e., motion of open curve and surface in 2D and 3D, respectively [10, 12]. It was also successfully extended for solving anisotropic surface diffusion with the Riemannian metric anisotropic surface energy [11, 13]. Recently, based on BGN’s variational formulation for surface diffusion, by approximating the normal vector in a clever way, Bao and Zhao [9, 4, 5] presented a structure-preserving PFEM (SP-PFEM) for surface diffusion, which preserves area/volume conservation in 2D/3D and unconditional energy dissipation at the discretized level.

Very recently, for the evolution of a closed curve under anisotropic surface diffusion in 2D, we proposed and analyzed an SP-PFEM for solving the anisotropic surface diffusion with a general anisotropic surface energy  $\gamma(\mathbf{n})$  [6]. The key ingredients for the new SP-PFEM are based on (i) introducing a proper symmetric and positive definite surface energy matrix depending on the Cahn–Hoffman  $\xi$ -vector and a stabilizing function, (ii) obtaining a new symmetrized (and conservative) geometric partial differential equations (PDEs) and its variational formulation for anisotropic surface diffusion with arbitrary surface energy in 2D, and (iii) representing the geometric PDEs and their variational formulation via the simple and natural arclength parametrization of a curve in 2D such that all the formulations are in the classical sense, and thus they are very simple and easy to understand, especially for nongeometers. Unfortunately, due to the adoption of the arclength parametrization in 2D and the local tangent space of a curve in 2D being one dimension (and thus the tangent

vector can be chosen as the natural basis of the local tangent space), many formulations in [6] for 2D cannot be extended to 3D straightforwardly and easily! In fact, to design and analyze an SP-PFEM for the evolution of a closed surface under anisotropic surface diffusion with a general anisotropic surface energy  $\gamma(\mathbf{n})$  in 3D is much more subtle and challenging than that in 2D, especially to establish the unconditional energy-dissipation property in the discretized level.

The main aim of this paper is to extend the SP-PFEM method recently proposed in [6] for 2D to 3D for the evolution of a closed surface under anisotropic surface diffusion with arbitrary surface energy. The key steps are (i) to introduce a proper symmetric and positive definite surface energy matrix  $Z_k(\mathbf{n})$  depending on the Cahn–Hoffman  $\xi$ -vector and a stabilizing function  $k(\mathbf{n}) : \mathbb{S}^2 \rightarrow \mathbb{R}$  as well as the anisotropic surface energy  $\gamma(\mathbf{n})$ , (ii) to formulate the geometric PDEs in 3D via the surface Laplace–Beltrami operator  $\Delta_S$ , the surface gradient operator  $\nabla_S$ , and the surface divergent operator  $\nabla_S \cdot$ , (iii) to obtain a new symmetrized (and conservative) variational formulation via different surface operators and the chemical potential  $\mu$  as well as the surface energy matrix  $Z_k(\mathbf{n})$ , (iv) to combine the SP-PFEM discretization techniques for anisotropic surface diffusion in 2D and isotropic surface diffusion in 3D, which were introduced in the literature [6, 9], and (v) to adapt several new techniques for proving the unconditional energy-dissipation property of the proposed SP-PFEM in 3D, which is the most difficult and challenging part of this paper. Under the simple and mild condition on the surface energy  $\gamma(\mathbf{n})$

$$(1.5) \quad \gamma(-\mathbf{n}) = \gamma(\mathbf{n}) \quad \forall \mathbf{n} \in \mathbb{S}^2, \quad \gamma \in C^2(\mathbb{R}^3 \setminus \{\mathbf{0}\}),$$

we successfully establish the two structure-preserving properties—volume conservation and energy dissipation—for the proposed SP-PFEM for anisotropic surface diffusion in 3D in the discretized level. In fact, to show the energy dissipation of the proposed SP-PFEM in 3D, we need to overcome a few more difficulties which only exist in 3D instead of 2D: (i) the functional introduced for showing the existence of a minimal stabilizing function is nonlinear in terms of  $k := k(\mathbf{n})$  in 3D, while it is linear in 2D; (ii) because the local tangent space of a surface in 3D is two dimensions, in the proof of the existence of a minimal stabilizing function, we need to handle  $\gamma(\mathbf{u} \times \mathbf{v})$  for any  $\mathbf{u}, \mathbf{v} \in \mathbb{S}^2$  and thus there is no lower positive bound of  $\gamma(\mathbf{u} \times \mathbf{v})$  because  $|\mathbf{u} \times \mathbf{v}|$  could be degenerated to 0, while there is a lower positive bound of  $\gamma(\mathbf{u})$  for  $\mathbf{u} \in \mathbb{S}^1$  in 2D; and (iii) a completely new approach to derive the minimal stabilizing function  $k_0(\mathbf{n})$  is needed due to the degeneracy in the energy estimate in 3D, while it is not degenerate and thus the inequality of arithmetic and geometric means (AM-GM inequality) can be applied directly in 2D. We furthermore remark here that all formulations in this paper are still valid in 2D and the proof is also valid in 2D. Of course, it might be much easier to read and understand [6] for the 2D case as readers do not need to have some basic geometric knowledge.

The paper is organized as follows. In section 2, we recall the mathematical representations for anisotropic surface diffusion, obtain a symmetrized variational formulation, and propose an SP-PFEM to discretize it. In section 3, we establish energy stability of the proposed SP-PFEM. Extensive numerical results are reported to demonstrate the efficiency and accuracy as well as structure-preserving properties in section 4. Finally, some conclusions are drawn in section 5.

## 2. A new symmetrized variational formulation and its discretization.

We begin with a mathematical representation for the anisotropic surface diffusion in 3D, introduce a symmetric positive surface energy matrix  $Z_k(\mathbf{n})$ , and obtain a

symmetrized conservative variational formulation for anisotropic surface diffusion in 3D. An SP-PFEM is presented to discretize the variational formulation and some structural preserving properties are established.

**2.1. Mathematical representations for anisotropic surface diffusion.** Let the closed and orientable surface  $S := S(t)$  be globally parameterized by  $\mathbf{X}(\boldsymbol{\rho}, t)$ ,

$$(2.1) \quad \mathbf{X}(t) : \Omega \rightarrow \mathbb{R}^3, \boldsymbol{\rho} \mapsto \mathbf{X}(\boldsymbol{\rho}, t) = (x_1(\boldsymbol{\rho}, t), x_2(\boldsymbol{\rho}, t), x_3(\boldsymbol{\rho}, t))^T,$$

where  $\Omega \subset \mathbb{R}^3$  is a fixed and closed surface. With respect to the definition of a global parametrization, we refer to [17, Definition 25]. Then the motion of  $S(t)$  under the anisotropic surface diffusion (1.1) can be mathematically described by the following geometric PDEs via the Cahn–Hoffman  $\xi$ -vector [24]:

$$(2.2) \quad \begin{cases} \partial_t \mathbf{X}(\boldsymbol{\rho}, t) = (\Delta_S \mu) \mathbf{n}, & \boldsymbol{\rho} \in \Omega, \quad t > 0, \\ \mu = \nabla_S \cdot \xi, \quad \xi = \nabla \gamma(\mathbf{p})|_{\mathbf{p}=\mathbf{n}}. \end{cases}$$

The anisotropic surface diffusion (2.2) can also be regarded as a geometric flow from the given initial closed and orientable surface  $S_0 := S(0) \subset \mathbb{R}^3$  to the surface  $S(t) \subset \mathbb{R}^3$ . We define the function spaces over the evolving surface  $S(t) = \mathbf{X}(\boldsymbol{\rho}, t)$ ,

$$(2.3) \quad L^2(S(t)) := \left\{ u : S(t) \rightarrow \mathbb{R} \mid \int_{S(t)} |u|^2 dA < \infty \right\},$$

equipped with the  $L^2$ -inner product

$$(2.4) \quad (u, v)_{S(t)} := \int_{S(t)} u v dA \quad \forall u, v \in L^2(S(t)).$$

We remark that the global parametrization is a diffeomorphism [17, Definition 25], thus  $L^2(S(t))$  is equivalent to  $L^2(\Omega)$ , i.e., independent of  $t$ , in the sense of diffeomorphism. The above inner product can be extended to  $[L^2(S(t))]^3$  by replacing the scalar product  $uv$  by the vector inner product  $\mathbf{u} \cdot \mathbf{v}$ . And we adopt the angle bracket to emphasize the inner product for two matrix-valued functions  $\mathbf{U}, \mathbf{V}$  in  $[L^2(S(t))]^{3 \times 3}$ ,

$$(2.5) \quad \langle \mathbf{U}, \mathbf{V} \rangle_{S(t)} := \int_{S(t)} \mathbf{U} : \mathbf{V} dA \quad \forall \mathbf{U}, \mathbf{V} \in [L^2(S(t))]^{3 \times 3},$$

where  $\mathbf{U} : \mathbf{V} = \text{Tr}(\mathbf{V}^T \mathbf{U})$  is the Frobenius inner product with  $\text{Tr}(\mathbf{U})$  denoting the trace of a matrix  $\mathbf{U} \in \mathbb{R}^{3 \times 3}$ . Furthermore, we introduce the Sobolev space

$$(2.6) \quad H^1(S(t)) := \left\{ u : S(t) \rightarrow \mathbb{R} \mid u \in L^2(S(t)), \nabla_S u \in [L^2(S(t))]^3 \right\}.$$

And this definition can be extended easily to  $[H^1(S(t))]^3$ . We adopt the notation  $\nabla_S f = (\underline{D}_1 f, \underline{D}_2 f, \underline{D}_3 f)^T$  for a scalar-valued function  $f$  [24], and the surface gradient for a vector-valued function  $\mathbf{F} = (f_1, f_2, f_3)^T$  is defined as

$$(2.7) \quad \nabla_S \mathbf{F} := (\nabla_S f_1, \nabla_S f_2, \nabla_S f_3)^T \in \mathbb{R}^{3 \times 3}.$$

**2.2. A new symmetrized variational formulation and its property.** Introducing the symmetric surface energy matrix  $\mathbf{Z}_k(\mathbf{n})$ ,

$$(2.8) \quad \begin{aligned} \mathbf{Z}_k(\mathbf{n}) &= \gamma(\mathbf{n}) I_3 - \mathbf{n} \xi^T(\mathbf{n}) - \xi(\mathbf{n}) \mathbf{n}^T + k(\mathbf{n}) \mathbf{n} \mathbf{n}^T \\ &= \gamma(\mathbf{n}) I_3 - \mathbf{n} \xi^T - \xi \mathbf{n}^T + k(\mathbf{n}) \mathbf{n} \mathbf{n}^T \quad \forall \mathbf{n} \in \mathbb{S}^2, \end{aligned}$$

where  $k(\mathbf{n}) : \mathbb{S}^2 \rightarrow \mathbb{R}^+$  is a stabilizing function which ensures  $\mathbf{Z}_k(\mathbf{n})$  is positive definite, it is easy to see that the above matrix is a direct generalization from 2D to 3D as proposed in [6]. Then we obtain a symmetric and conservative variational (weak) formulation for the chemical potential (or weighted mean curvature)  $\mu$  via the matrix  $\mathbf{Z}_k(\mathbf{n})$ . We remark here that, in the 2D case, we can obtain both a strong (PDE) and a weak (variational) formulation for the chemical potential (or weighted curvature)  $\mu$ ; however, in the 3D case, it is not easy to write a simple strong (PDE) formulation for the chemical potential (or weighted mean curvature)  $\mu$  via the matrix  $\mathbf{Z}_k(\mathbf{n})$ .

LEMMA 2.1 (the weak formulation for  $\mu$ ). *The weighted mean curvature  $\mu$  satisfies the following weak formulation:*

$$(2.9) \quad (\mu, \mathbf{n} \cdot \boldsymbol{\omega})_S = \langle \mathbf{Z}_k(\mathbf{n}) \nabla_S \mathbf{X}, \nabla_S \boldsymbol{\omega} \rangle_S \quad \forall \boldsymbol{\omega} = (\omega_1, \omega_2, \omega_3)^T \in [H^1(S(t))]^3.$$

*Proof.* Noticing the fact  $\underline{D}_i x_k = \delta_{i,k} - n_k n_i$  and  $\nabla_S f \cdot \mathbf{n} = 0$  [24], we obtain

$$(2.10) \quad \nabla_S x_k \cdot \nabla_S \omega_l = \sum_{i=1}^3 (\delta_{i,k} - n_k n_i) \underline{D}_i \omega_l = \underline{D}_k \omega_l - n_k \nabla_S \omega_l \cdot \mathbf{n} = \underline{D}_k \omega_l.$$

From [24, equation (8.18)], we know that

$$(2.11) \quad \int_{S(t)} \mu \mathbf{n} \cdot \boldsymbol{\omega} dA = - \sum_{k,l=1}^3 \int_S \xi_k n_l \underline{D}_k \omega_l dA + \sum_{k,l=1}^3 \int_S \gamma(\mathbf{n}) \underline{D}_k x_l \underline{D}_k \omega_l dA.$$

Substituting the identity (2.10) into [24, equation (8.18)] yields the following identity:

$$(2.12) \quad (\mu, \mathbf{n} \cdot \boldsymbol{\omega})_S = \gamma(\mathbf{n}) \sum_{l=1}^3 \int_{S(t)} \nabla_S x_l \cdot \nabla_S \omega_l dS - \sum_{k,l=1}^3 \int_{S(t)} \xi_k n_l \nabla_S x_k \cdot \nabla_S \omega_l dS.$$

Obviously, the second term  $\langle \gamma(\mathbf{n}) \nabla_S \mathbf{X}, \nabla_S \boldsymbol{\omega} \rangle_S$  corresponds to  $\gamma(\mathbf{n}) I_3$  in  $\mathbf{Z}_k(\mathbf{n})$ . Now by simplifying the last term, we have

$$\begin{aligned} \sum_{k,l=1}^3 \int_S \xi_k n_l \nabla_S x_k \cdot \nabla_S \omega_l dA &= \int_S \left( \sum_{k=1}^3 \xi_k (\nabla_S x_k) \right) \cdot \left( \sum_{l=1}^3 n_l (\nabla_S \omega_l) \right) dA \\ &= \int_S ((\nabla_S \mathbf{X})^T \boldsymbol{\xi}) \cdot ((\nabla_S \boldsymbol{\omega})^T \mathbf{n}) dA \\ &= \int_S \text{Tr}((\nabla_S \boldsymbol{\omega})^T \mathbf{n} \boldsymbol{\xi}^T (\nabla_S \mathbf{X})) dA \\ &= \int_S (\mathbf{n} \boldsymbol{\xi}^T (\nabla_S \mathbf{X})) : (\nabla_S \boldsymbol{\omega}) dA \\ (2.13) \quad &= \langle \mathbf{n} \boldsymbol{\xi}^T \nabla_S \mathbf{X}, \nabla_S \boldsymbol{\omega} \rangle_S, \end{aligned}$$

which is the  $\mathbf{n} \boldsymbol{\xi}^T(\mathbf{n})$  part in  $\mathbf{Z}_k(\mathbf{n})$ .

Finally, recalling the identity  $\nabla_S \mathbf{X} = I_3 - \mathbf{n} \mathbf{n}^T$  and combining the two identities (2.12) and (2.13) yields

$$\begin{aligned} (2.14) \quad (\mu, \mathbf{n} \cdot \boldsymbol{\omega})_S &= \langle (\gamma(\mathbf{n}) I_3 - \mathbf{n} \boldsymbol{\xi}^T) \nabla_S \mathbf{X}, \nabla_S \boldsymbol{\omega} \rangle_S \\ &= \langle \mathbf{Z}_k(\mathbf{n}) \nabla_S \mathbf{X}, \nabla_S \boldsymbol{\omega} \rangle_S + \langle (\boldsymbol{\xi} \mathbf{n}^T - k(\mathbf{n}) \mathbf{n} \mathbf{n}^T)(I_3 - \mathbf{n} \mathbf{n}^T), \nabla_S \boldsymbol{\omega} \rangle_S \\ &= \langle \mathbf{Z}_k(\mathbf{n}) \nabla_S \mathbf{X}, \nabla_S \boldsymbol{\omega} \rangle_S, \end{aligned}$$

which is the desired result.  $\square$

With the weak formulation of  $\mu$  (2.9) given in Lemma 2.1, by taking integration by parts, we can easily derive the following variational formulation for the anisotropic surface diffusion (2.2) (or (1.1)): For a given closed and orientable initial surface  $S(0) := S_0$ , find the solution  $(\mathbf{X}(\cdot, t), \mu(\cdot, t)) \in [H^1(S(t))]^3 \times H^1(S(t))$  such that

$$(2.15a) \quad (\partial_t \mathbf{X} \cdot \mathbf{n}, \psi)_{S(t)} + (\nabla_S \mu, \nabla_S \psi)_{S(t)} = 0 \quad \forall \psi \in H^1(S(t)),$$

$$(2.15b) \quad (\mu \mathbf{n}, \boldsymbol{\omega})_{S(t)} - \langle \mathbf{Z}_k(\mathbf{n}) \nabla_S \mathbf{X}, \nabla_S \boldsymbol{\omega} \rangle_{S(t)} = 0 \quad \forall \boldsymbol{\omega} \in [H^1(S(t))]^3.$$

Denote the enclosed volume and the free energy of  $S(t)$  as  $V(t)$  and  $W(t)$ , respectively, which are defined by

$$(2.16) \quad V(t) := \frac{1}{3} \int_{S(t)} \mathbf{X} \cdot \mathbf{n} dA, \quad W(t) := \int_{S(t)} \gamma(\mathbf{n}) dA.$$

We then show the two geometric properties still hold for the variational formulation (2.15).

**THEOREM 2.2.** *The enclosed volume  $V(t)$  and the free energy  $W(t)$  of the solution  $S(t)$  of the variational formulation (2.15) are conserved and dissipative, respectively.*

*Proof.* Taking the derivative of  $V(t)$  with respect to  $t$ , from [42], we know that

$$(2.17) \quad \frac{dV(t)}{dt} = \int_{S(t)} V_n dA = (\partial_t \mathbf{X} \cdot \mathbf{n}, 1)_{S(t)} = 0, \quad t \geq 0,$$

which implies volume conservation.

Similarly, the derivative of  $W(t)$  with respect to  $t$  is

$$(2.18) \quad \frac{dW(t)}{dt} = \int_{S(t)} V_n \mu dA = (\partial_t \mathbf{X} \cdot \mathbf{n}, \mu)_{S(t)} = -(\nabla_S \mu, \nabla_S \mu)_{S(t)} \leq 0, \quad t \geq 0,$$

which implies energy dissipation.  $\square$

**2.3. A structure-preserving parametric finite element method.** We take  $\tau > 0$  to be the time step size, and the discrete time levels are  $t_m = m\tau$  for each  $m \geq 0$ . For spatial discretization, as illustrated in Figure 2.1, the orientable surface  $S(t_m)$  is approximated by an orientable polyhedron  $S^m = \cup_{j=1}^J \bar{\sigma}_j^m$  with  $J$  mutually disjoint nondegenerated triangles surfaces  $\sigma_j^m$  and  $I$  vertices  $\mathbf{q}_i^m$ . We further denote  $\{\mathbf{q}_{j_1}^m, \mathbf{q}_{j_2}^m, \mathbf{q}_{j_3}^m\}$  as the three ordered vertices of the triangle  $\sigma_j^m$ , the induced orientation vector  $\mathcal{J}\{\sigma_j^m\} := (\mathbf{q}_{j_2}^m - \mathbf{q}_{j_1}^m) \times (\mathbf{q}_{j_3}^m - \mathbf{q}_{j_2}^m)$ , and the outward unit normal vector  $\mathbf{n}_j^m$  of  $\sigma_j^m$  are thus given by  $\mathbf{n}_j^m = \frac{\mathcal{J}\{\sigma_j^m\}}{|\mathcal{J}\{\sigma_j^m\}|}$ . We refer the definition of the orientable polyhedron to Definition 47 in [17].

The finite element space with respect to the orientable surface  $S^m = \cup_{j=1}^J \bar{\sigma}_j^m$  is defined as

$$(2.19) \quad \mathbb{K}^m := \left\{ u \in C(S^m) \mid u|_{\sigma_j^m} \in \mathcal{P}^1(\sigma_j^m) \ \forall 1 \leq j \leq J \right\},$$

which is equipped with the mass lumped inner product  $(\cdot, \cdot)_{S^m}^h$  with  $h$  denoting the mesh size of  $S^m$  as

$$(2.20) \quad (f, g)_{S^m}^h := \frac{1}{3} \sum_{j=1}^J \sum_{i=1}^3 |\sigma_j^m| f((\mathbf{q}_{j_i}^m)^-) g((\mathbf{q}_{j_i}^m)^-),$$

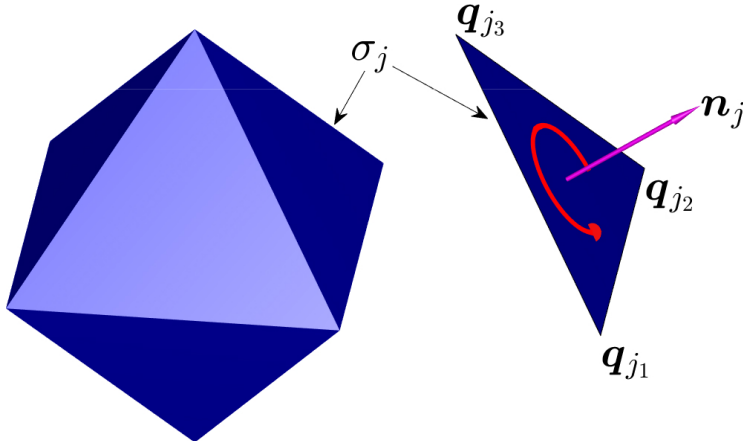


FIG. 2.1. An illustration of the approximation polyhedron  $S^0$ . The vertices  $\{q_{j_1}, q_{j_2}, q_{j_3}\}$  of the triangle  $\sigma_j$  are oriented counterclockwise; see the red circular arrow. The direction of the normal vector  $n_j$  is determined by the right-hand rule.

where  $\mathcal{P}^1(\sigma_j^m)$  is the space of polynomials on  $\sigma_j^m$  with degree at most 1,  $|\sigma_j^m| := \frac{1}{2}|\mathcal{J}\{\sigma_j^m\}|$  denotes the area of  $\sigma_j^m$ , and  $f((q_{j_i}^m)^-)$  means the one-sided limit of  $f(\mathbf{x})$  at  $q_{j_i}^m$  inside  $\sigma_j^m$ . This definition is also valid for vector- and matrix-valued functions, and the mass lumped inner product of the matrix-valued functions  $\mathbf{U}$  and  $\mathbf{V}$  is also emphasized by the angle bracket as

$$(2.21) \quad \langle \mathbf{U}, \mathbf{V} \rangle_{S^m}^h := \frac{1}{3} \sum_{j=1}^J \sum_{i=1}^3 |\sigma_j^m| \mathbf{U}((q_{j_i}^m)^-) : \mathbf{V}((q_{j_i}^m)^-).$$

We remark here that  $(f, g)_{S^m}^h$  and  $\langle \mathbf{U}, \mathbf{V} \rangle_{S^m}^h$  can be viewed as approximations of  $(f, g)_{S^m}$  and  $\langle \mathbf{U}, \mathbf{V} \rangle_{S^m}$ , respectively. Finally, the discretized surface gradient operator  $\nabla_S$  for  $f \in \mathbb{K}^m$  is given by

$$(2.22) \quad \nabla_S f|_{\sigma_j^m} := \left( f(q_{j_1}^m)(q_{j_2}^m - q_{j_3}^m) + f(q_{j_2}^m)(q_{j_3}^m - q_{j_1}^m) + f(q_{j_3}^m)(q_{j_1}^m - q_{j_2}^m) \right) \times \frac{n_j^m}{|\mathcal{J}\{\sigma_j^m\}|},$$

and for vector-valued function  $\mathbf{F} = (f_1, f_2, f_3)^T \in [\mathbb{K}^m]^3$ ,  $\nabla_S \mathbf{F} := (\nabla_S f_1, \nabla_S f_2, \nabla_S f_3)^T$ .

By using the PFEM for spatial discretization and adapting an implicit-explicit (IMEX) Euler method for temporal discretization, i.e., linear parts via the backward Euler method and a nonlinear part via the backward Euler method with proper linearization as well as the integration limits via the forward Euler method, an IMEX SP-PFEM for the variational formulation (2.15) can then be stated as follows: Given the initial approximation  $S^0 = \cup_{j=1}^J \overline{\sigma_j^0}$  of  $S(0)$ ; for each time step  $t_m = m\tau$  ( $m \geq 0$ ), find the solution  $(\mathbf{X}^{m+1}, \mu^{m+1}) \in [\mathbb{K}^m]^3 \times \mathbb{K}^m$  such that

$$(2.23a) \quad \left( \frac{\mathbf{X}^{m+1} - \mathbf{X}^m}{\tau} \cdot \mathbf{n}^{m+\frac{1}{2}}, \psi \right)_{S^m} + (\nabla_S \mu^{m+1}, \nabla_S \psi)_{S^m} = 0 \quad \forall \psi \in \mathbb{K}^m,$$

$$(2.23b) \quad \left( \mu^{m+1} \mathbf{n}^{m+\frac{1}{2}}, \boldsymbol{\omega} \right)_{S^m} - \langle \mathbf{Z}_k(\mathbf{n}^m) \nabla_S \mathbf{X}^{m+1}, \nabla_S \boldsymbol{\omega} \rangle_{S^m} = 0 \quad \forall \boldsymbol{\omega} \in [\mathbb{K}^m]^3.$$

Here  $\mathbf{X}^m(\mathbf{q}_i^m) = \mathbf{q}_i^m$ ,  $\mathbf{X}^{m+1}(\mathbf{q}_i^m) = \mathbf{q}_i^{m+1}$  for each  $i$ ,  $\mathbf{n}^m|_{\sigma_j^m} = \mathbf{n}_j^m$ ,  $\sigma_j^{m+1} = \mathbf{X}^{m+1}(\sigma_j^m)$  is the triangle with ordered vertices  $\{\mathbf{q}_{j_1}^{m+1}, \mathbf{q}_{j_2}^{m+1}, \mathbf{q}_{j_3}^{m+1}\}$  for each  $j$ , and  $S^{m+1} = \cup_{j=1}^J \bar{\sigma}_j^{m+1}$  for each  $m$ . The semi-implicit approximation  $\mathbf{n}^{m+\frac{1}{2}}$  of the outward normal vector  $\mathbf{n}$  at  $t = (m + \frac{1}{2})\tau$  is defined as follows:

$$(2.24) \quad \mathbf{n}^{m+\frac{1}{2}}|_{\sigma_j^m} := \frac{\mathcal{J}\{\sigma_j^m\} + 4\mathcal{J}\{\sigma_j^{m+\frac{1}{2}}\} + \mathcal{J}\{\sigma_j^{m+1}\}}{6|\mathcal{J}\{\sigma_j^m\}|},$$

where  $\sigma_j^{m+\frac{1}{2}} := \frac{1}{2}(\sigma_j^m + \sigma_j^{m+1})$ .

*Remark 2.1.* We note the function  $\mathbf{X}^{m+1}$  has different meanings at time step  $t_m$  (as a function in  $[\mathbb{K}^m]^3$ ) and  $t_{m+1}$  (as a function in  $[\mathbb{K}^{m+1}]^3$ ), and we adopt the same notation for simplicity.

**2.4. Main results.** For the discretized polygon surface  $S^m = \cup_{j=1}^J \bar{\sigma}_j^m$ , its enclosed volume and surface energy are denoted as  $V^m$  and  $W^m$ , respectively, which are defined as

$$(2.25a) \quad V^m := \frac{1}{3} \int_{S^m} \mathbf{X}^m \cdot \mathbf{n}^m dA = \frac{1}{9} \sum_{j=1}^J \sum_{i=1}^3 |\sigma_j^m| \mathbf{q}_{ji}^m \cdot \mathbf{n}_j^m,$$

$$(2.25b) \quad W^m := \int_{S^m} \gamma(\mathbf{n}^m) dA = \sum_{j=1}^J |\sigma_j^m| \gamma(\mathbf{n}_j^m) \quad \forall m \geq 0.$$

Denote the auxiliary function  $F_k(\mathbf{n}, \mathbf{u}, \mathbf{v}) : [\mathbb{S}^2]^3 \rightarrow \mathbb{R}$  as

$$(2.26) \quad F_k(\mathbf{n}, \mathbf{u}, \mathbf{v}) := (\mathbf{u}^T \mathbf{Z}_k(\mathbf{n}) \cdot \mathbf{u})(\mathbf{v}^T \mathbf{Z}_k(\mathbf{n}) \cdot \mathbf{v}),$$

and define the minimal stabilizing function  $k_0(\mathbf{n}) : \mathbb{S}^2 \rightarrow \mathbb{R}$  as (its existence will be given in the next section)

$$(2.27) \quad k_0(\mathbf{n}) = \inf \left\{ k(\mathbf{n}) \mid F_k(\mathbf{n}, \mathbf{u}, \mathbf{v}) \geq \gamma^2(\mathbf{u} \times \mathbf{v}) \quad \forall \mathbf{u}, \mathbf{v} \in \mathbb{S}^2 \right\}.$$

Then for the SP-PFEM (2.23), we have the following.

**THEOREM 2.3** (structural-preserving). *Assume  $\gamma(\mathbf{n})$  satisfies (1.5) and take  $k(\mathbf{n})$  in (2.8) satisfying  $k(\mathbf{n}) \geq k_0(\mathbf{n})$  for  $\mathbf{n} \in \mathbb{S}^2$ ; then the SP-PFEM (2.23) is volume conservation and energy dissipation, i.e.,*

$$(2.28a) \quad V^{m+1} = V^m = \dots = V^0 \quad \forall m \geq 0,$$

$$(2.28b) \quad W^{m+1} \leq W^m \leq \dots \leq W^0 \quad \forall m \geq 0.$$

The proof of volume conservation (2.28a) relies on the key identity  $V^{m+1} - V^m = ((\mathbf{X}^{m+1} - \mathbf{X}^m) \cdot \mathbf{n}^{m+\frac{1}{2}}, \psi)_{S^m}$ , which can be found in [9] and thus the proof is omitted here for brevity, and we will establish the energy dissipation or unconditional energy stability (2.28b) in the next section.

*Remark 2.2.* The SP-PFEM (2.23) is “weakly” implicit, i.e., at each time step, one needs to solve a nonlinear coupled system, which can be solved efficiently by the Newton’s method. Of course, if we simply replace  $\mathbf{n}^{m+\frac{1}{2}}$  in (2.23) by  $\mathbf{n}^m$ , we can obtain an ES-PFEM, where only a linear system needs to be solved at each time. Of course for the semi-implicit ES-PFEM, the volume conservation is no longer valid.

Under the same condition as in Theorem 2.3, the ES-PFEM is also unconditionally energy stable.

*Remark 2.3.* The semidiscretization of the variational problem (2.15) in space by the PFEM also preserves the two geometric properties. And the proof is similar to the isotropic case; for details, we refer to [10, 50, 9].

*Remark 2.4.* We remark here that all formulations in this section are still valid in 2D. In fact, assume  $S(t)$  to be a closed curve in 2D with unit outward normal vector  $\mathbf{n} \in \mathbb{S}^1$  and tangent vector  $\boldsymbol{\tau} = \mathbf{n}^\perp$ , where  $^\perp$  denotes the clockwise rotation by  $\frac{\pi}{2}$ , and assume  $S(t)$  to be globally parameterized by  $\mathbf{X}(\rho, t) : \mathbb{R}/\mathbb{Z} \rightarrow \mathbb{R}^2$  [6]. We further assume  $s$  to be the arclength parameter of the closed curve  $S(t)$  and thus  $\boldsymbol{\tau} = \partial_s \mathbf{X}(\rho, t)$  [6]. Notice that

$$\nabla_S = \boldsymbol{\tau} \partial_s, \quad \Delta_S = (\boldsymbol{\tau} \partial_s) \cdot (\boldsymbol{\tau} \partial_s) = \partial_{ss}, \quad \nabla_S \mathbf{X} = \partial_s \mathbf{X} \boldsymbol{\tau}^T;$$

then we have

$$\Delta_S \mu = \partial_{ss} \mu, \quad \nabla_S \cdot \boldsymbol{\xi} = \boldsymbol{\tau} \cdot \partial_s \boldsymbol{\xi} = \mathbf{n}^\perp \cdot \partial_s \boldsymbol{\xi} = -\mathbf{n} \cdot \partial_s \boldsymbol{\xi}^\perp,$$

$$(\nabla_S \mu, \nabla_S \psi)_{S(t)} = (\boldsymbol{\tau} \partial_s \mu, \boldsymbol{\tau} \partial_s \psi)_{S(t)} = (\partial_s \mu, \partial_s \psi)_{S(t)},$$

$$\begin{aligned} \langle \mathbf{Z}_k(\mathbf{n}) \nabla_S \mathbf{X}, \nabla_S \boldsymbol{\omega} \rangle_{S(t)} &= \langle \mathbf{Z}_k(\mathbf{n}) \partial_s \mathbf{X} \boldsymbol{\tau}^T, \partial_s \boldsymbol{\omega} \boldsymbol{\tau}^T \rangle_{S(t)} \\ &= \int_{S(t)} \text{Tr}(\boldsymbol{\tau} \partial_s \boldsymbol{\omega}^T \mathbf{Z}_k(\mathbf{n}) \partial_s \mathbf{X} \boldsymbol{\tau}^T) dA \\ &= \int_{S(t)} \text{Tr}(\partial_s \boldsymbol{\omega}^T \mathbf{Z}_k(\mathbf{n}) \partial_s \mathbf{X} \boldsymbol{\tau}^T \boldsymbol{\tau}) dA \\ &= (\mathbf{Z}_k(\mathbf{n}) \partial_s \mathbf{X}, \partial_s \boldsymbol{\omega})_{S(t)}. \end{aligned}$$

Thus the above equations (2.2) and (2.15) collapse to (1.5) and (2.11) in [6], respectively, in the corresponding 2D setup.

**3. Energy stability.** In this section, we first prove the existence of  $k_0(\mathbf{n})$  and show its sublinear property as a functional of  $\gamma(\mathbf{n})$ . By utilizing the existence of  $k_0(\mathbf{n})$  together with several lemmas, we finally prove the energy stability part of our main theorem, (2.28b).

**3.1. Minimal stabilizing function.** From (2.27), we know that  $F_{k_0}(\mathbf{n}, \mathbf{u}, \mathbf{v}) \geq 0$ . Taking  $k = k_0$ ,  $\mathbf{u} = \mathbf{n}$ , and  $\mathbf{v} = \boldsymbol{\tau} \in \mathbb{S}^2$  satisfying  $\boldsymbol{\tau} \cdot \mathbf{n} = 0$  in (2.26), noticing  $\boldsymbol{\tau}^T \mathbf{Z}_{k_0}(\mathbf{n}) \boldsymbol{\tau} = \gamma(\mathbf{n}) > 0$  and  $\mathbf{n} \cdot \boldsymbol{\xi} = \gamma(\mathbf{n})$ , we obtain

$$(3.1) \quad 0 \leq \mathbf{n}^T \mathbf{Z}_{k_0}(\mathbf{n}) \mathbf{n} = k_0(\mathbf{n}) - \gamma(\mathbf{n}) \Rightarrow k_0(\mathbf{n}) \geq \gamma(\mathbf{n}) > 0, \quad \mathbf{n} \in \mathbb{S}^2.$$

To prove the existence of  $k_0(\mathbf{n})$ , for any given  $\mathbf{n} \in \mathbb{S}^2$ , we only need to show there exists a  $k(\mathbf{n})$  sufficiently large such that  $F_k(\mathbf{n}, \mathbf{u}, \mathbf{v}) \geq \gamma^2(\mathbf{u} \times \mathbf{v})$  for any  $\mathbf{u}, \mathbf{v} \in \mathbb{S}^2$ .

LEMMA 3.1. *Let  $G(\mathbf{n}, \mathbf{u}, \mathbf{v})$  be an auxiliary function given by*

$$(3.2) \quad G(\mathbf{n}, \mathbf{u}, \mathbf{v}) := \gamma(\mathbf{n}) [\gamma(\mathbf{n}) - 2(\boldsymbol{\xi} \cdot \mathbf{u})(\mathbf{n} \cdot \mathbf{u}) - 2(\boldsymbol{\xi} \cdot \mathbf{v})(\mathbf{n} \cdot \mathbf{v})], \quad \mathbf{n}, \mathbf{u}, \mathbf{v} \in \mathbb{S}^2;$$

*then for any  $k(\mathbf{n}) > 0$ , the following inequality holds:*

$$(3.3) \quad F_k(\mathbf{n}, \mathbf{u}, \mathbf{v}) - G(\mathbf{n}, \mathbf{u}, \mathbf{v}) \geq [\gamma(\mathbf{n}) k(\mathbf{n}) - 4|\boldsymbol{\xi}|^2] [( \mathbf{n} \cdot \mathbf{u})^2 + (\mathbf{n} \cdot \mathbf{v})^2].$$

*Proof.* By direct computation and the arithmetic-geometric mean inequality, we obtain

$$\begin{aligned} & F_k(\mathbf{n}, \mathbf{u}, \mathbf{v}) - G(\mathbf{n}, \mathbf{u}, \mathbf{v}) \\ & \geq \gamma(\mathbf{n})k(\mathbf{n})[(\mathbf{n} \cdot \mathbf{u})^2 + (\mathbf{n} \cdot \mathbf{v})^2] + k(\mathbf{n})^2(\mathbf{n} \cdot \mathbf{u})^2(\mathbf{n} \cdot \mathbf{v})^2 \\ & \quad - 4|\xi|^2|(\mathbf{n} \cdot \mathbf{u})(\mathbf{n} \cdot \mathbf{v})| - 2|\xi|k(\mathbf{n})|(\mathbf{n} \cdot \mathbf{u})(\mathbf{n} \cdot \mathbf{v})|(|\mathbf{n} \cdot \mathbf{u}| + |\mathbf{n} \cdot \mathbf{v}|) \\ & \geq [\gamma(\mathbf{n})k(\mathbf{n}) - 2|\xi|^2][(n \cdot u)^2 + (n \cdot v)^2] + k(n)^2(n \cdot u)^2(n \cdot v)^2 \\ & \quad - k(n)|\xi|\left[(n \cdot u)^2\left(\frac{2|\xi|}{k(n)} + \frac{k(n)}{2|\xi|}(n \cdot v)^2\right) + (n \cdot v)^2\left(\frac{2|\xi|}{k(n)} + \frac{k(n)}{2|\xi|}(n \cdot u)^2\right)\right] \\ & = [\gamma(\mathbf{n})k(\mathbf{n}) - 4|\xi|^2][(n \cdot u)^2 + (n \cdot v)^2], \end{aligned}$$

which is the desired inequality (3.3).  $\square$

Since  $\gamma(\mathbf{p})$  is not differentiable at  $\mathbf{0}$ , in order to handle  $\gamma^2(\mathbf{u} \times \mathbf{v})$ , we first show the following lemma.

LEMMA 3.2. *For any  $\gamma(\mathbf{n})$  satisfying (1.5), then  $\gamma^2(\mathbf{p})$  is continuous differentiable in  $\mathbb{R}^3$ . Moreover, there exists a constant  $C_1$  defined by*

$$(3.4) \quad C_1 = \frac{1}{2} \sup_{\mathbf{n} \in \mathbb{S}^2} \|\mathbf{H}_{\gamma^2}(\mathbf{n})\|_2, \quad \mathbf{H}_{\gamma^2}(\mathbf{n}) = \nabla \nabla \gamma^2(\mathbf{p})|_{\mathbf{p}=\mathbf{n}},$$

where  $\|\cdot\|_2$  is the spectral norm, such that

$$(3.5) \quad \gamma^2(\mathbf{p}) - \gamma^2(\mathbf{q}) \leq \nabla(\gamma^2(\mathbf{q})) \cdot (\mathbf{p} - \mathbf{q}) + C_1|\mathbf{p} - \mathbf{q}|^2 \quad \forall \mathbf{p}, \mathbf{q} \in \mathbb{R}^3.$$

*Proof.* It is straightforward to check  $\gamma^2(\mathbf{p}) \in C^1(\mathbb{R}^3)$  by definition.

To prove the inequality (3.5), we first consider the case that the line segment of  $\mathbf{p}, \mathbf{q}$  does not pass  $\mathbf{0}$ , i.e.,  $\lambda \mathbf{p} + (1 - \lambda) \mathbf{q} \neq \mathbf{0}$  for all  $0 \leq \lambda \leq 1$ . Since  $\gamma^2(\mathbf{p})$  is homogeneous of degree 2, we know that  $\mathbf{H}_{\gamma^2}(\mathbf{p})$  is homogeneous of degree 0, which yields

$$(3.6) \quad \mathbf{H}_{\gamma^2}(\zeta) = \mathbf{H}_{\gamma^2}(\zeta/|\zeta|) \quad \forall \mathbf{0} \neq \zeta \in \mathbb{R}^3.$$

By the mean value theorem, there exists a  $\lambda_0 \in (0, 1)$  and  $\zeta = \lambda_0 \mathbf{p} + (1 - \lambda_0) \mathbf{q} \neq \mathbf{0}$  such that

$$(3.7) \quad \gamma^2(\mathbf{p}) = \gamma^2(\mathbf{q}) + \nabla(\gamma^2(\mathbf{q})) \cdot (\mathbf{p} - \mathbf{q}) + \frac{1}{2}(\mathbf{p} - \mathbf{q})^T \mathbf{H}_{\gamma^2}(\zeta)(\mathbf{p} - \mathbf{q}).$$

Thus (3.5) holds for such  $\mathbf{p}, \mathbf{q}$ .

If  $\mathbf{0}$  is contained in the line segment of  $\mathbf{p}, \mathbf{q}$ , we can find a sequence  $(\mathbf{p}_k, \mathbf{q}_k) \rightarrow (\mathbf{p}, \mathbf{q})$  such that for each  $k$ , the line segment of  $\mathbf{p}_k, \mathbf{q}_k$  does not pass  $\mathbf{0}$ . We know (3.5) holds for such  $\mathbf{p}_k, \mathbf{q}_k$ . By using the continuity of  $\gamma^2(\mathbf{p})$  and  $\nabla(\gamma^2(\mathbf{p}))$ , we obtain that (3.5) is valid in this case by letting  $k \rightarrow \infty$ .

Thus the inequality (3.5) is established.  $\square$

THEOREM 3.3. *Suppose  $\gamma(\mathbf{n})$  satisfies the energy stability condition (1.5). Then there exists a constant  $K(\mathbf{n}) < \infty$  that only depends on  $\gamma(\mathbf{n})$  given by*

$$(3.8) \quad K := K(\mathbf{n}) = \frac{6|\xi(\mathbf{n})|^2 + 8\gamma(\mathbf{n})|\xi(\mathbf{n})| + 16C_1}{\gamma(\mathbf{n})} < \infty \quad \forall \mathbf{n} \in \mathbb{S}^2$$

such that  $F_K(\mathbf{n}, \mathbf{u}, \mathbf{v}) \geq \gamma^2(\mathbf{u} \times \mathbf{v})$  for any  $\mathbf{u}, \mathbf{v} \in \mathbb{S}^2$ .

*Proof.* It is convenient to first consider the special case  $\mathbf{n} = (0, 0, 1)^T$ . For any  $\mathbf{u}, \mathbf{v} \in \mathbb{S}^2$ , we write them in the spherical coordinates as

$$(3.9a) \quad \mathbf{u} = (\cos \theta_1 \cos \phi_1, \sin \theta_1 \cos \phi_1, \sin \phi_1)^T, \quad 0 \leq \theta_1 < 2\pi, \quad -\frac{\pi}{2} \leq \phi_1 \leq \frac{\pi}{2},$$

$$(3.9b) \quad \mathbf{v} = (\cos \theta_2 \cos \phi_2, \sin \theta_2 \cos \phi_2, \sin \phi_2)^T, \quad 0 \leq \theta_2 < 2\pi, \quad -\frac{\pi}{2} \leq \phi_2 \leq \frac{\pi}{2},$$

where in the case when  $\phi_1 = \pm\frac{\pi}{2}$ , we choose  $\theta_1 = 0$ , and when  $\phi_2 = \pm\frac{\pi}{2}$ , we choose  $\theta_2 = 0$ . The cross product  $\mathbf{u} \times \mathbf{v}$  is then represented as

$$(3.10) \quad \mathbf{u} \times \mathbf{v} = \cos \phi_2 \sin \phi_1 \hat{\mathbf{v}}_0 + \cos \phi_1 \sin \phi_2 \hat{\mathbf{u}}_0 + \cos \phi_1 \cos \phi_2 \hat{\mathbf{w}}_0,$$

where

$$\begin{aligned} \hat{\mathbf{u}}_0 &= (\sin \theta_1, -\cos \theta_1, 0)^T, & \hat{\mathbf{v}}_0 &= (-\sin \theta_2, \cos \theta_2, 0)^T, \\ \hat{\mathbf{w}}_0 &= (0, 0, \sin \theta_{21})^T \quad \text{with } \theta_{21} = \theta_2 - \theta_1, \end{aligned}$$

since  $\mathbf{u}, \mathbf{v}$  are symmetric in  $F_K(\mathbf{n}, \mathbf{u}, \mathbf{v})$  and  $\gamma^2(\mathbf{u} \times \mathbf{v})$ . Without loss of generality, we can always assume  $\sin \theta_{21} \geq 0$ .

Denoting  $\mathbf{u}_0, \mathbf{v}_0 \in \mathbb{S}^2$  as

$$(3.11) \quad \mathbf{u}_0 := (\cos \theta_1, \sin \theta_1, 0)^T, \quad \mathbf{v}_0 := (\cos \theta_2, \sin \theta_2, 0)^T,$$

we know that  $|(\mathbf{u} - \mathbf{u}_0) \times \mathbf{v}| \leq |\mathbf{u} - \mathbf{u}_0|, |\mathbf{u} \times (\mathbf{v} - \mathbf{v}_0)| \leq |\mathbf{v} - \mathbf{v}_0|, |(\mathbf{u} - \mathbf{u}_0) \times (\mathbf{v} - \mathbf{v}_0)| \leq |\mathbf{u} - \mathbf{u}_0| + |\mathbf{v} - \mathbf{v}_0|$  since  $|\mathbf{u}|, |\mathbf{v}|, |\mathbf{u}_0|, |\mathbf{v}_0| = 1$ . Thus we get

$$(3.12) \quad |\mathbf{u} \times \mathbf{v} - \mathbf{u}_0 \times \mathbf{v}_0|^2 \leq 8(|\mathbf{u} - \mathbf{u}_0|^2 + |\mathbf{v} - \mathbf{v}_0|^2).$$

Taking  $\mathbf{p} = \mathbf{u} \times \mathbf{v}, \mathbf{q} = \mathbf{u}_0 \times \mathbf{v}_0$  in (3.5), and noticing  $\mathbf{u}_0 \times \mathbf{v}_0 = (\sin \theta_{21}) \mathbf{n}$ , we obtain

$$\begin{aligned} &\gamma^2(\mathbf{u} \times \mathbf{v}) - (\sin \theta_{21})^2 \gamma^2(\mathbf{n}) \\ &\leq \sin \theta_{21} \nabla(\gamma^2(\mathbf{n})) \cdot (\mathbf{u} \times \mathbf{v} - \mathbf{u}_0 \times \mathbf{v}_0) + C_1 |\mathbf{u} \times \mathbf{v} - \mathbf{u}_0 \times \mathbf{v}_0|^2 \\ &\leq 2\gamma(\mathbf{n}) \xi \cdot (\sin \phi_1 \hat{\mathbf{v}}_0 + \sin \phi_2 \hat{\mathbf{u}}_0) \sin \theta_{21} \\ &\quad + 2\gamma(\mathbf{n}) \xi \cdot ((\cos \phi_2 - 1) \sin \phi_1 \mathbf{v}_0 + (\cos \phi_1 - 1) \sin \phi_2 \mathbf{u}_0) \sin \theta_{21} \\ &\quad + 2\gamma(\mathbf{n}) \xi \cdot \hat{\omega}_0 (1 - \cos \phi_1 \cos \phi_2) \sin \theta_{21} + 8C_1 (|\mathbf{u} - \mathbf{u}_0|^2 + |\mathbf{v} - \mathbf{v}_0|^2) \\ &\leq 2\gamma(\mathbf{n}) \xi \cdot [(\cos \theta_{21} \mathbf{v}_0 - \mathbf{u}_0) (\mathbf{n} \cdot \mathbf{u}) + (\cos \theta_{21} \mathbf{u}_0 - \mathbf{v}_0) (\mathbf{n} \cdot \mathbf{v})] \\ (3.13) \quad &\quad + 4(\gamma(\mathbf{n}) |\xi| + 4C_1) [(\mathbf{n} \cdot \mathbf{u})^2 + (\mathbf{n} \cdot \mathbf{v})^2]. \end{aligned}$$

Here we use the facts  $|\mathbf{u} - \mathbf{u}_0| = 2|\sin \frac{\phi_1}{2}|, |\mathbf{v} - \mathbf{v}_0| = 2|\sin \frac{\phi_2}{2}|, (\sin \phi)^2 \geq 2(\sin \frac{\phi}{2})^2 = 1 - \cos \phi$  for all  $-\frac{\pi}{2} \leq \phi \leq \frac{\pi}{2}$ , and  $0 \leq 1 - \cos \phi_1 \cos \phi_2 \leq (1 - \cos \phi_1) + (1 - \cos \phi_2)$ .

To estimate  $G(\mathbf{n}, \mathbf{u}, \mathbf{v})$ , we observe the following inequalities:

$$\begin{aligned} (3.14a) \quad (\xi \cdot \mathbf{u})(\mathbf{n} \cdot \mathbf{u}) &= (\xi \cdot \mathbf{u}_0)(\mathbf{n} \cdot \mathbf{u}) + (\xi \cdot (\mathbf{u} - \mathbf{u}_0))(\mathbf{n} \cdot (\mathbf{u} - \mathbf{u}_0)) \\ &\leq (\xi \cdot \mathbf{u}_0)(\mathbf{n} \cdot \mathbf{u}) + |\xi| |\mathbf{u} - \mathbf{u}_0|^2 \\ &\leq (\xi \cdot \mathbf{u}_0)(\mathbf{n} \cdot \mathbf{u}) + 2|\xi| (\mathbf{n} \cdot \mathbf{u})^2, \end{aligned}$$

$$(3.14b) \quad (\xi \cdot \mathbf{v})(\mathbf{n} \cdot \mathbf{v}) \leq (\xi \cdot \mathbf{v}_0)(\mathbf{n} \cdot \mathbf{v}) + 2|\xi| (\mathbf{n} \cdot \mathbf{v})^2.$$

Combining (3.2) and (3.14) yields

$$\begin{aligned} (3.15) \quad G(\mathbf{n}, \mathbf{u}, \mathbf{v}) &= \gamma^2(\mathbf{n}) - 2\gamma(\mathbf{n}) [(\xi \cdot \mathbf{u})(\mathbf{n} \cdot \mathbf{u}) + (\xi \cdot \mathbf{v})(\mathbf{n} \cdot \mathbf{v})] \\ &\geq \gamma^2(\mathbf{n}) - 2\gamma(\mathbf{n}) [(\xi \cdot \mathbf{u}_0)(\mathbf{n} \cdot \mathbf{u}) + (\xi \cdot \mathbf{u}_0)(\mathbf{n} \cdot \mathbf{u})] \\ &\quad - 4\gamma(\mathbf{n}) |\xi| [(\mathbf{n} \cdot \mathbf{u})^2 + (\mathbf{n} \cdot \mathbf{v})^2]. \end{aligned}$$

Finally, by (3.3) in Lemma 3.1, the estimation of  $\gamma^2(\mathbf{u} \times \mathbf{v})$  in (3.13), and the estimation of  $G(\mathbf{n}, \mathbf{u}, \mathbf{v})$  in (3.15), we obtain

$$\begin{aligned} & F_K(\mathbf{n}, \mathbf{u}, \mathbf{v}) - \gamma^2(\mathbf{u} \times \mathbf{v}) \\ & \geq \gamma(\mathbf{n})^2 (\cos \theta_{21})^2 - 2\gamma(\mathbf{n}) \cos \theta_{21} [(\boldsymbol{\xi} \cdot \mathbf{v}_0)(\mathbf{n} \cdot \mathbf{u}) + (\boldsymbol{\xi} \cdot \mathbf{u}_0)(\mathbf{n} \cdot \mathbf{v})] \\ & \quad + [\gamma(\mathbf{n})K(\mathbf{n}) - 4|\boldsymbol{\xi}|^2 - 8\gamma(\mathbf{n})|\boldsymbol{\xi}| - 16C_1] [(\mathbf{n} \cdot \mathbf{u})^2 + (\mathbf{n} \cdot \mathbf{v})^2] \\ & \geq \gamma(\mathbf{n})^2 (\cos \theta_{21})^2 - 2\gamma(\mathbf{n}) |\cos \theta_{21}| |\boldsymbol{\xi}| [(\mathbf{n} \cdot \mathbf{u}) + (\mathbf{n} \cdot \mathbf{v})] \\ & \quad + 2|\boldsymbol{\xi}|^2 [(\mathbf{n} \cdot \mathbf{u})^2 + (\mathbf{n} \cdot \mathbf{v})^2] \\ & \geq 0. \end{aligned}$$

Thus we have  $F_K(\mathbf{n}, \mathbf{u}, \mathbf{v}) \geq \gamma^2(\mathbf{u} \times \mathbf{v})$  for the special case  $\mathbf{n} = (0, 0, 1)^T$ .

Since the constant  $K(\mathbf{n})$  only depends on  $\gamma(\mathbf{n})$ , the proof is valid for arbitrary  $\mathbf{n} \in \mathbb{S}^2$  via a similar argument. The proof is completed.  $\square$

Theorem 3.3 indicates that the set  $\{k(\mathbf{n}) | F_k(\mathbf{n}, \mathbf{u}, \mathbf{v}) \geq \gamma^2(\mathbf{u} \times \mathbf{v}) \text{ for all } \mathbf{u}, \mathbf{v} \in \mathbb{S}^2\}$  contains at least an element  $K(\mathbf{n}) < \infty$ , and thus it is not empty. This, together with the fact  $k_0(\mathbf{n}) \geq \gamma(\mathbf{n})$ , yields the existence of the minimal stabilizing function  $k_0(\mathbf{n})$ .

**COROLLARY 3.4** (existence of the minimal stabilizing function). *Suppose the surface energy  $\gamma(\mathbf{n})$  satisfies the energy-stable condition (1.5). Then the minimal stabilizing function  $k_0(\mathbf{n})$  in (2.27) is well-defined.*

Finally, we point out the minimal stabilizing function  $k_0(\mathbf{n})$  is determined by  $\gamma(\mathbf{n})$ , and thus we can consider the mapping from  $\gamma(\mathbf{n})$  to  $k_0(\mathbf{n})$ . Similar to the result in 2D in [6], the mapping is sublinear.

**THEOREM 3.5** (positive homogeneity and subadditivity). *Let  $k_0(\mathbf{n})$ ,  $k_1(\mathbf{n})$ , and  $k_2(\mathbf{n})$  be the minimal stabilizing functions of  $\gamma(\mathbf{n})$ ,  $\gamma_1(\mathbf{n})$ , and  $\gamma_2(\mathbf{n})$ , respectively. Then we have*

- (i) *for any  $c > 0$ ,  $ck_0(\mathbf{n})$  is the stabilizing function of  $c\gamma(\mathbf{n})$ , and*
- (ii) *suppose  $\gamma(\mathbf{n}) = \gamma_1(\mathbf{n}) + \gamma_2(\mathbf{n})$ , then  $k_0(\mathbf{n}) \leq k_1(\mathbf{n}) + k_2(\mathbf{n})$  for  $\mathbf{n} \in \mathbb{S}^2$ .*

*Proof.* The proof of positive homogeneity in (i) is similar to the proof of Lemma 4.4 in [6], and thus details are omitted here for brevity.

To prove the subadditivity in (ii), we denote

$$\boldsymbol{\xi} := \nabla \gamma(\mathbf{p})|_{\mathbf{p}=\mathbf{n}}, \quad \boldsymbol{\xi}_1 := \nabla \gamma_1(\mathbf{p})|_{\mathbf{p}=\mathbf{n}}, \quad \boldsymbol{\xi}_2 := \nabla \gamma_2(\mathbf{p})|_{\mathbf{p}=\mathbf{n}}.$$

Since  $k_1(\mathbf{n})$  is the minimal stabilizing function of  $\gamma_1(\mathbf{n})$ , for any  $t \in \mathbb{R}$ , we have

$$\begin{aligned} & \frac{1}{2} \mathbf{u}^T \mathbf{Z}_{k_1}(\mathbf{n}) \mathbf{u} + \frac{t^2}{2} \mathbf{v}^T \mathbf{Z}_{k_1}(\mathbf{n}) \mathbf{v} - t\gamma_1(\mathbf{u} \times \mathbf{v}) \\ & \geq 2\sqrt{\frac{t^2}{4} F_{k_1}(\mathbf{n}, \mathbf{u}, \mathbf{v}) - t\gamma_1(\mathbf{u} \times \mathbf{v})} \\ (3.16) \quad & \geq 0 \quad \forall \mathbf{n}, \mathbf{u}, \mathbf{v} \in \mathbb{S}^2. \end{aligned}$$

A similar inequality is also true for  $\gamma_2(\mathbf{n})$ . Adding the two inequalities together and noticing  $\boldsymbol{\xi} = \boldsymbol{\xi}_1 + \boldsymbol{\xi}_2$ , we obtain

$$(3.17) \quad \frac{1}{2} \mathbf{u}^T \mathbf{Z}_{k_1+k_2}(\mathbf{n}) \mathbf{u} + \frac{t^2}{2} \mathbf{v}^T \mathbf{Z}_{k_1+k_2}(\mathbf{n}) \mathbf{v} - t\gamma(\mathbf{u} \times \mathbf{v}) \geq 0, \quad \forall t \in \mathbb{R},$$

which means its discriminant  $\gamma^2(\mathbf{u} \times \mathbf{v}) - F_{k_1+k_2}(\mathbf{n}, \mathbf{u}, \mathbf{v}) \leq 0$  for all  $\mathbf{n}, \mathbf{u}, \mathbf{v} \in \mathbb{S}^2$ . Then the subadditivity is a direct conclusion from the definition of the minimal stabilizing function (2.27).  $\square$

**3.2. Proof of the main theorem.** By establishing the existence of  $k_0(\mathbf{n})$ , we now have enough tools to prove (2.28b) in Theorem 2.3. To simplify the proof, we first introduce the following alternative definition for the surface gradient operator  $\nabla_S$ .

LEMMA 3.6. Suppose  $\sigma$  be a nondegenerated triangle with three ordered vertices  $\{\mathbf{q}_1, \mathbf{q}_2, \mathbf{q}_3\}$  (cf. Figure 2.1). Let  $f$  and  $\mathbf{F}$  be scalar- and vector-valued functions in  $\mathcal{P}^1(\sigma)/[\mathcal{P}^1(\sigma)]^3$ , respectively, and  $\{\mathbf{n}, \boldsymbol{\tau}_1, \boldsymbol{\tau}_2\}$  forms an orthonormal basis. Then the discretized surface gradient operator  $\nabla_S$  in (2.22) satisfies

$$(3.18) \quad \nabla_S f = (\partial_{\boldsymbol{\tau}_1} f) \boldsymbol{\tau}_1 + (\partial_{\boldsymbol{\tau}_2} f) \boldsymbol{\tau}_2, \quad \nabla_S \mathbf{F} = (\partial_{\boldsymbol{\tau}_1} \mathbf{F}) \boldsymbol{\tau}_1^T + (\partial_{\boldsymbol{\tau}_2} \mathbf{F}) \boldsymbol{\tau}_2^T,$$

where  $\partial_{\boldsymbol{\tau}} f$  denotes the directional derivative of  $f$  with respect to  $\boldsymbol{\tau}$ .

*Proof.* It suffices to prove the left equality in (3.18). Let  $\mathbf{x} = \lambda_1 \mathbf{q}_1 + \lambda_2 \mathbf{q}_2 + \lambda_3 \mathbf{q}_3$  with  $0 \leq \lambda_1, \lambda_2, \lambda_3 \leq 1$  satisfying  $\lambda_1 + \lambda_2 + \lambda_3 = 1$  be a point in  $\sigma$ . We observe that

$$\begin{aligned} [(\mathbf{q}_3 - \mathbf{q}_2) \times \mathbf{n}] \cdot (\mathbf{x} - \mathbf{q}_3) &= [(\mathbf{x} - \mathbf{q}_3) \times (\mathbf{q}_3 - \mathbf{q}_2)] \cdot \mathbf{n} \\ &= [(-\lambda_1(\mathbf{q}_3 - \mathbf{q}_1) - \lambda_2(\mathbf{q}_3 - \mathbf{q}_2)) \times (\mathbf{q}_3 - \mathbf{q}_2)] \cdot \mathbf{n} \\ &= -\lambda_1 [(\mathbf{q}_2 - \mathbf{q}_1 + \mathbf{q}_3 - \mathbf{q}_2) \times (\mathbf{q}_3 - \mathbf{q}_2)] \cdot \mathbf{n} \\ (3.19) \quad &= -\lambda_1 |\mathcal{J}\{\sigma\}|. \end{aligned}$$

Thus  $\lambda_1 = \frac{(\mathbf{q}_2 - \mathbf{q}_3) \times \mathbf{n}}{|\mathcal{J}\{\sigma\}|} \cdot (\mathbf{x} - \mathbf{q}_3)$ , and  $\lambda_2, \lambda_3$  can be derived similarly.

By the definition of the directional derivative, we deduce that

$$\begin{aligned} \partial_{\boldsymbol{\tau}_1} f(\mathbf{x}) &= \lim_{h \rightarrow 0} \frac{f(\mathbf{x} + h\boldsymbol{\tau}_1) - f(\mathbf{x})}{h} \\ &= \lim_{h \rightarrow 0} \frac{1}{h} \left( f(\mathbf{q}_1) \frac{(\mathbf{q}_2 - \mathbf{q}_3) \times \mathbf{n}}{|\mathcal{J}\{\sigma\}|} \cdot (h\boldsymbol{\tau}_1) \right. \\ &\quad \left. + f(\mathbf{q}_2) \frac{(\mathbf{q}_3 - \mathbf{q}_1) \times \mathbf{n}}{|\mathcal{J}\{\sigma\}|} \cdot (h\boldsymbol{\tau}_1) + f(\mathbf{q}_3) \frac{(\mathbf{q}_1 - \mathbf{q}_2) \times \mathbf{n}}{|\mathcal{J}\{\sigma\}|} \cdot (h\boldsymbol{\tau}_1) \right) \\ (3.20) \quad &= \nabla_S f(\mathbf{x}) \cdot \boldsymbol{\tau}_1. \end{aligned}$$

Similarly, we have  $\partial_{\boldsymbol{\tau}_2} f = \nabla_S f \cdot \boldsymbol{\tau}_2$ . Since  $\{\mathbf{n}, \boldsymbol{\tau}_1, \boldsymbol{\tau}_2\}$  forms an orthognormal basis, by vector decomposition and  $\nabla_S f \cdot \mathbf{n} = 0$ , we obtain

$$\begin{aligned} \nabla_S f &= (\nabla_S f \cdot \mathbf{n}) \mathbf{n} + (\nabla_S f \cdot \boldsymbol{\tau}_1) \boldsymbol{\tau}_1 + (\nabla_S f \cdot \boldsymbol{\tau}_2) \boldsymbol{\tau}_2 \\ (3.21) \quad &= (\partial_{\boldsymbol{\tau}_1} f) \boldsymbol{\tau}_1 + (\partial_{\boldsymbol{\tau}_2} f) \boldsymbol{\tau}_2, \end{aligned}$$

which is the desired identity.  $\square$

With the help of (3.18), we can then give the following upper bound of the summand  $\gamma(\mathbf{n}) |\sigma|$  in the discretized energy  $W^m$  in (2.25b).

LEMMA 3.7. Suppose  $\sigma$  and  $\bar{\sigma}$  are two nondegenerated triangles with ordered vertices  $\{\mathbf{q}_1, \mathbf{q}_2, \mathbf{q}_3\}, \{\bar{\mathbf{q}}_1, \bar{\mathbf{q}}_2, \bar{\mathbf{q}}_3\}$ , and outward unit normal vectors  $\mathbf{n}$  and  $\bar{\mathbf{n}}$ , respectively (cf. Figure 2.1). Let  $\mathbf{X}$  be a vector-valued function in  $[\mathcal{P}^1(\sigma)]^3$  satisfying  $\mathbf{X}(\mathbf{q}_i) = \bar{\mathbf{q}}_i$  for  $i = 1, 2, 3$ . Then for any  $k(\mathbf{n}) \geq k_0(\mathbf{n})$  for  $\mathbf{n} \in \mathbb{S}^2$ , the following inequality holds:

$$(3.22) \quad \frac{1}{6} |\sigma| \sum_{i=1}^3 (\mathbf{Z}_k(\mathbf{n}) \nabla_S \mathbf{X}((\mathbf{q}_i)^-)) : \nabla_S \mathbf{X}((\mathbf{q}_i)^-) \geq \gamma(\bar{\mathbf{n}}) |\bar{\sigma}|.$$

*Proof.* Since  $\mathbf{X} \in [\mathcal{P}^1(\sigma)]^3$ , its derivative  $\nabla_S \mathbf{X}$  is a constant matrix in  $\sigma$ . Suppose  $\{\mathbf{n}, \boldsymbol{\tau}_1, \boldsymbol{\tau}_2\}$  forms an orthonormal basis; by applying (3.18), we obtain

$$(3.23) \quad \nabla_S \mathbf{X}((\mathbf{q}_i)^-) = (\partial_{\boldsymbol{\tau}_1} \mathbf{X}((\mathbf{q}_i)^-)) \boldsymbol{\tau}_1^T + (\partial_{\boldsymbol{\tau}_2} \mathbf{X}((\mathbf{q}_i)^-)) \boldsymbol{\tau}_2^T, \quad i = 1, 2, 3.$$

Let  $\partial_{\tau_1} \mathbf{X} = s\mathbf{u}$  and  $\partial_{\tau_2} \mathbf{X} = t\mathbf{v}$  with  $s, t \geq 0$  and  $\mathbf{u}, \mathbf{v} \in \mathbb{S}^2$ . Substituting this and the definition of  $Z_k(\mathbf{n})$  in (2.8) into the left-hand side of (3.22), we get

$$\begin{aligned} & \frac{1}{6} |\sigma| \sum_{i=1}^3 (\mathbf{Z}_k(\mathbf{n}) \nabla_S \mathbf{X}((\mathbf{q}_i)^-)) : \nabla_S \mathbf{X}((\mathbf{q}_i)^-) \\ &= \frac{1}{2} |\sigma| (\mathbf{Z}_k(\mathbf{n}) (s\mathbf{u}\tau_1^T + t\mathbf{v}\tau_2^T)) : (s\mathbf{u}\tau_1^T + t\mathbf{v}\tau_2^T) \\ &= \frac{1}{2} |\sigma| (s^2 (\boldsymbol{\tau}_1 \cdot \boldsymbol{\tau}_1) \mathbf{u}^T \mathbf{Z}_k(\mathbf{n}) \mathbf{u} + t^2 (\boldsymbol{\tau}_2 \cdot \boldsymbol{\tau}_2) \mathbf{v}^T \mathbf{Z}_k(\mathbf{n}) \mathbf{v}) \\ (3.24) \quad &\geq st |\sigma| \sqrt{F_k(\mathbf{n}, \mathbf{u}, \mathbf{v})} \geq st |\sigma| \gamma(\mathbf{u} \times \mathbf{v}). \end{aligned}$$

For the right-hand side of (3.22), since  $\bar{\sigma} = \mathbf{X}(\sigma)$ , it holds that

$$(3.25) \quad \gamma(\bar{\mathbf{n}}) |\bar{\sigma}| = \gamma(\bar{\mathbf{n}}) \int_{\sigma} |(\partial_{\tau_1} \mathbf{X}) \times (\partial_{\tau_2} \mathbf{X})| dA = st |\sigma| \gamma(\bar{\mathbf{n}}) |\mathbf{u} \times \mathbf{v}|.$$

Finally, since  $\mathbf{X} \in [\mathcal{P}^1(\sigma)]^3$ , for  $\mathbf{p}$  and  $\mathbf{p} + h\boldsymbol{\tau}_1$  in  $\sigma$ , we have  $\mathbf{X}(\mathbf{p} + h\boldsymbol{\tau}_1)$  and  $\mathbf{X}(\mathbf{p})$  in  $\bar{\sigma}$ . From the definition of directional derivative for functions in  $[\mathcal{P}^1(\sigma)]^3$ , we get

$$(3.26) \quad s \mathbf{u} \cdot \bar{\mathbf{n}} = (\partial_{\tau_1} \mathbf{X}) \cdot \bar{\mathbf{n}} = \frac{\mathbf{X}(\mathbf{p} + h\boldsymbol{\tau}_1) - \mathbf{X}(\mathbf{p})}{h} \cdot \bar{\mathbf{n}} = 0,$$

and similarly  $\mathbf{v} \cdot \bar{\mathbf{n}} = 0$ , thus  $\gamma(\mathbf{u} \times \mathbf{v}) = |\mathbf{u} \times \mathbf{v}| \gamma(\bar{\mathbf{n}})$ . This equation, together with (3.24) and (3.25), yields the desired inequality (3.22).  $\square$

With the help of Lemma 3.7, we can then prove the energy stability part (2.28b) in our main theorem, Theorem 2.3.

*Proof.* First for any  $\mathbf{p} \in \mathbb{S}^2$ , since  $k(\mathbf{n}) \geq k_0(\mathbf{n})$ , we have

$$(3.27) \quad \mathbf{p}^T \mathbf{Z}_k(\mathbf{n}) \mathbf{p} = \gamma(\mathbf{n}) - 2(\boldsymbol{\xi} \cdot \mathbf{p})(\mathbf{n} \cdot \mathbf{p}) + k(\mathbf{n})(\mathbf{n} \cdot \mathbf{p})^2 \geq 0,$$

thus  $\mathbf{Z}_k(\mathbf{n})$  is positive definite. By Cauchy's inequality, it holds that

$$\begin{aligned} & \langle \mathbf{Z}_k(\mathbf{n}^m) \nabla_S \mathbf{X}^{m+1}, \nabla_S (\mathbf{X}^{m+1} - \mathbf{X}^m) \rangle_{S^m}^h \\ (3.28) \quad &\geq \frac{1}{2} \langle \mathbf{Z}_k(\mathbf{n}^m) \nabla_S \mathbf{X}^{m+1}, \nabla_S \mathbf{X}^{m+1} \rangle_{S^m}^h - \frac{1}{2} \langle \mathbf{Z}_k(\mathbf{n}^m) \nabla_S \mathbf{X}^m, \nabla_S \mathbf{X}^m \rangle_{S^m}^h. \end{aligned}$$

Suppose  $\{\mathbf{n}_j^m, \boldsymbol{\tau}_{j,1}^m, \boldsymbol{\tau}_{j,2}^m\}$  ( $1 \leq j \leq J$ ) forms an orthonormal basis; by using (3.18), we obtain

$$\begin{aligned} & \frac{1}{2} \langle \mathbf{Z}_k(\mathbf{n}^m) \nabla_S \mathbf{X}^m, \nabla_S \mathbf{X}^m \rangle_{S^m}^h \\ &= \frac{1}{6} \sum_{j=1}^J \sum_{i=1}^3 |\sigma_j^m| \left( \mathbf{Z}_k(\mathbf{n}_j^m) \nabla_S \mathbf{X}^m ((\mathbf{q}_{j,i}^m)^-) \Big|_{\sigma_j^m} \right) : \left( \nabla_S \mathbf{X}^m ((\mathbf{q}_{j,i}^m)^-) \Big|_{\sigma_j^m} \right) \\ &= \frac{1}{2} \sum_{j=1}^J |\sigma_j^m| [(\boldsymbol{\tau}_{j,1}^m)^T \mathbf{Z}_k(\mathbf{n}_j^m) \boldsymbol{\tau}_{j,1}^m + (\boldsymbol{\tau}_{j,2}^m)^T \mathbf{Z}_k(\mathbf{n}_j^m) \boldsymbol{\tau}_{j,2}^m] \\ &= \frac{1}{2} \sum_{j=1}^J |\sigma_j^m| \gamma(\mathbf{n}_j^m) (\boldsymbol{\tau}_{j,1}^m \cdot \boldsymbol{\tau}_{j,1}^m + \boldsymbol{\tau}_{j,2}^m \cdot \boldsymbol{\tau}_{j,2}^m) \\ (3.29) \quad &= \sum_{j=1}^J |\sigma_j^m| \gamma(\mathbf{n}_j^m) = W^m. \end{aligned}$$

For  $1 \leq j \leq J$ , applying Lemma 3.7 with  $\sigma = \sigma_j^m$ ,  $\bar{\sigma} = \sigma_j^{m+1}$ , and  $\mathbf{X} = \mathbf{X}^{m+1}|_{\sigma_j^m}$ , we get

$$(3.30) \quad \frac{1}{6} |\sigma_j^m| \sum_{j=1}^3 \left( \mathbf{Z}_k(\mathbf{n}_j^m) \nabla_S \mathbf{X}^m ((\mathbf{q}_{j_i}^m)^-) |_{\sigma_j^m} \right) : \left( \nabla_S \mathbf{X}^m ((\mathbf{q}_{j_i}^m)^-) |_{\sigma_j^m} \right) \geq \gamma(\mathbf{n}_j^{m+1}) |\sigma_j^{m+1}|.$$

Summing (3.30) for  $j = 1, 2, \dots, J$  and combining (3.28) and (3.29), we obtain

$$(3.31) \quad \begin{aligned} & \langle \mathbf{Z}_k(\mathbf{n}^m) \nabla_S \mathbf{X}^{m+1}, \nabla_S (\mathbf{X}^{m+1} - \mathbf{X}^m) \rangle_{S^m}^h + W^m \\ & \geq \frac{1}{2} \langle \mathbf{Z}_k(\mathbf{n}^m) \nabla_S \mathbf{X}^{m+1}, \nabla_S \mathbf{X}^{m+1} \rangle_{S^m}^h \\ & \geq W^{m+1}, \quad m \geq 0. \end{aligned}$$

Finally, choosing  $\psi = \mu^{m+1}$  in (2.23a) and  $\omega = \mathbf{X}^{m+1}$  in (2.23b), noting (3.31), we have

$$(3.32) \quad W^{m+1} - W^m \leq \tau \langle \nabla_S \mu^{m+1}, \nabla_S \mu^{m+1} \rangle_{S^m}^h \leq 0, \quad m \geq 0,$$

which immediately implies the unconditional energy stability (2.28b) in Theorem 2.3.  $\square$

*Remark 3.1.* We remark here that if in 2D, the inequality (3.31) is replaced by [6, (4.22)]

$$(3.33) \quad \frac{1}{2} \langle \mathbf{Z}_k(\mathbf{n}^m) \nabla_S \mathbf{X}^{m+1}, \nabla_S \mathbf{X}^{m+1} \rangle_{S^m}^h + \frac{1}{2} W^m \geq W^{m+1}.$$

Due to the additional positive term  $\frac{1}{2} W^m$  on the left-hand side of the above inequality, the proof can much simplified and is straightforward by using the AM-GM inequality [6].

**4. Numerical results.** In this section, we first state the setup for solving the SP-PFEM (2.23). Then we present several numerical computations, including the convergence test and the structure-preserving test. Finally, we apply (2.23) to simulate surface evolution for different anisotropic energies.

In our practical computations, the minimal stabilizing function  $k_0(\mathbf{n})$  can be obtained via numerically solving (2.27). Then by taking a stabilizing function  $k(\mathbf{n}) \geq k_0(\mathbf{n})$  for  $\mathbf{n} \in \mathbb{S}^2$ , we can determine the surface energy matrix  $\mathbf{Z}_k(\mathbf{n})$ , and thus the SP-PFEM (2.23) is well-determined. At each time step, the weakly nonlinear system (2.23) is solved by the Newton's method with a given tolerance at  $\varepsilon_0 = 10^{-12}$  [9].

Given an initial closed surface  $S_0$ , we generate its approximation  $S^0 := S_0^h = \cup_{j=1}^J \overline{\sigma_j^0}$  with  $J$  triangles  $\{\sigma_j^0\}_{j=1}^J$  and  $I$  vertices  $\{\mathbf{q}_i^0\}_{i=1}^I$  by using the MATLAB toolbox called *CFDTool* [40] with a given parameter mesh size  $h$ . Given a time step size  $\tau$  and a mesh size  $h$ , we denote  $(\mathbf{X}_{h,\tau}^m, \mu_{h,\tau}^m)$  as the solution of (2.23) with the initial approximation  $S_0^h$  at the time  $t = t_m$ . We define  $\mathbf{X}_{h,\tau}(t)$  by

$$(4.1) \quad \mathbf{X}_{h,\tau}(\cdot, t) = \frac{t - t_m}{\tau} \mathbf{X}_{h,\tau}^m(\cdot) + \frac{t_{m+1} - t}{\tau} \mathbf{X}_{h,\tau}^{m+1}(\cdot) \quad \forall t \in [t_m, t_{m+1}], \quad m \geq 0,$$

and the surface  $S_{h,\tau}(t)$  is represented by  $\mathbf{X}_{h,\tau}(\cdot, t)$ .

To test the convergence rate of (2.23), we adopt the manifold distance  $M(\cdot, \cdot)$  to measure the difference between two closed surfaces  $S_1$  and  $S_2$ , which is given by

$$(4.2) \quad M(S_1, S_2) := 2|\Omega_1 \cup \Omega_2| - |\Omega_1| - |\Omega_2|,$$

where  $\Omega_1$  and  $\Omega_2$  are the regions enclosed by  $S_1$  and  $S_2$ , respectively, and  $|\Omega|$  denotes the volume of the region  $\Omega$ . Based on the manifold distance, the numerical error is defined as

$$(4.3) \quad e_{h,\tau}(t) := M(S_{h,\tau}(t), S(t)), \quad t \geq 0.$$

TABLE 4.1

Numerical errors of  $e_{h,\tau}(t=0.5)$  and  $e_{h,\tau}(t=1)$  for Cases 1–6, while  $h_0 := 2^{-1}$  and  $\tau_0 := \frac{2}{25}^{-1}$  with 140 triangles and 72 vertices for the initial partition  $S_0^{h_0}$ , with 624 triangles and 314 vertices for the initial partition  $S_0^{h_0/2}$ , and with 2502 triangles and 1253 vertices for the initial partition  $S_0^{h_0/4}$ .

$(h, \tau)$	$e_{h,\tau}(\frac{1}{2})$ Case 1	Order	$e_{h,\tau}(\frac{1}{2})$ Case 2	Order	$e_{h,\tau}(\frac{1}{2})$ Case 3	Order
$(h_0, \tau_0)$	1.24E-1	-	1.47E-1	-	1.12E-1	-
$(\frac{h_0}{2}, \frac{\tau_0}{4})$	3.06E-2	2.01	3.54E-2	2.05	2.82E-2	1.98
$(\frac{h_0}{2^2}, \frac{\tau_0}{4^2})$	7.90E-3	1.96	8.74E-3	2.02	7.54E-3	1.90
$(h, \tau)$	$e_{h,\tau}(\frac{1}{2})$ Case 4	Order	$e_{h,\tau}(\frac{1}{2})$ Case 5	Order	$e_{h,\tau}(\frac{1}{2})$ Case 6	Order
$(h_0, \tau_0)$	1.10E-1	-	1.12E-1	-	1.12E-1	-
$(\frac{h_0}{2}, \frac{\tau_0}{4})$	2.83E-2	1.96	2.89E-2	1.96	3.09E-2	1.99
$(\frac{h_0}{2^2}, \frac{\tau_0}{4^2})$	7.48E-3	1.92	7.58E-3	1.93	7.86E-3	1.97
$(h, \tau)$	$e_{h,\tau}(1)$ Case 1	Order	$e_{h,\tau}(1)$ Case 2	Order	$e_{h,\tau}(1)$ Case 3	Order
$(h_0, \tau_0)$	1.46E-1	-	1.22E-1	-	1.11E-1	-
$(\frac{h_0}{2}, \frac{\tau_0}{4})$	3.52E-2	2.05	3.01E-2	2.02	2.74E-2	2.02
$(\frac{h_0}{2^2}, \frac{\tau_0}{4^2})$	8.67E-3	2.02	7.75E-3	1.96	7.21E-3	1.93
$(h, \tau)$	$e_{h,\tau}(1)$ Case 4	Order	$e_{h,\tau}(1)$ Case 5	Order	$e_{h,\tau}(1)$ Case 6	Order
$(h_0, \tau_0)$	1.10E-1	-	1.10E-1	-	1.13E-1	-
$(\frac{h_0}{2}, \frac{\tau_0}{4})$	2.76E-2	1.99	2.80E-2	1.97	2.90E-2	1.96
$(\frac{h_0}{2^2}, \frac{\tau_0}{4^2})$	7.23E-3	1.93	7.36E-3	1.93	7.56E-3	1.94

In our practical computations,  $S(t)$  is obtained numerically by taking  $k(\mathbf{n}) = k_0(\mathbf{n})$  and with a very refined mesh size at  $h = h_e = 2^{-4}$  and a very small time step at  $\tau = \tau_e = \frac{2}{25}h_e^2$ .

In the numerical experiments for testing convergence rates, the time step size and the mesh size are chosen as  $\tau = \frac{2}{25}h^2$ , the initial shape  $S_0$  is chosen as a  $2 \times 2 \times 1$  cuboid, and its finest partition is a polyhedron  $S_0^{h_e}$  with 10718 triangles and 5361 vertices. We consider the following five cases of the anisotropic surface energy  $\gamma(\mathbf{n})$  as well as the stabilizing function  $k(\mathbf{n})$ :

- Case 1:  $\gamma(\mathbf{n}) = 1 + \frac{1}{4}(n_1^4 + n_2^4 + n_3^4)$ ,  $k(\mathbf{n}) = k_0(\mathbf{n})$ ;
- Case 2:  $\gamma(\mathbf{n}) = 1 + \frac{1}{2}(n_1^4 + n_2^4 + n_3^4)$ ,  $k(\mathbf{n}) = k_0(\mathbf{n})$ ;
- Case 3:  $\gamma(\mathbf{n}) = (n_1^4 + n_2^4 + n_3^4)^{\frac{1}{4}}$ ,  $k(\mathbf{n}) = k_0(\mathbf{n})$ ;
- Case 4:  $\gamma(\mathbf{n}) = (n_1^4 + n_2^4 + n_3^4)^{\frac{1}{4}}$ ,  $k(\mathbf{n}) = k_0(\mathbf{n}) + 1$ ;
- Case 5:  $\gamma(\mathbf{n}) = (n_1^4 + n_2^4 + n_3^4)^{\frac{1}{4}}$ ,  $k(\mathbf{n}) = k_0(\mathbf{n}) + 2$ ;
- Case 6:  $\gamma(\mathbf{n}) = (n_1^4 + n_2^4 + n_3^4)^{\frac{1}{4}}$ ,  $k(\mathbf{n}) = k_0(\mathbf{n}) + 5$ .

The numerical errors are listed in Table 4.1. We note that while  $\gamma(\mathbf{n})$  and  $k(\mathbf{n})$  are chosen differently in different cases, the convergence rates for this manifold error are all about second order in  $h$ . These results indicate that the proposed SP-PFEM (2.23) has a good robustness in convergence rate, which is in general independent of  $\gamma(\mathbf{n})$  and  $k(\mathbf{n})$ . Thus in practical computations, there is no need to choose  $k(\mathbf{n})$  as the minimal stabilizing function  $k_0(\mathbf{n})$ .

To examine the volume conservation and unconditional energy dissipation, we consider these two indicators: the normalized volume change  $\frac{\Delta V(t)}{V(0)} := \frac{V(t) - V(0)}{V(0)}$  and the normalized energy  $\frac{W(t)}{W(0)}$ . The initial shape is taken as a  $2 \times 2 \times 1$  ellipsoid. Figure 4.1 shows the normalized volume change  $\frac{\Delta V(t)}{V(0)}$  for Cases 1–3 with fixed  $h = 2^{-3}$  and  $\tau = \frac{2}{25}h^2$ . We find the order of magnitude of the volume change  $\Delta V(t)$  is at

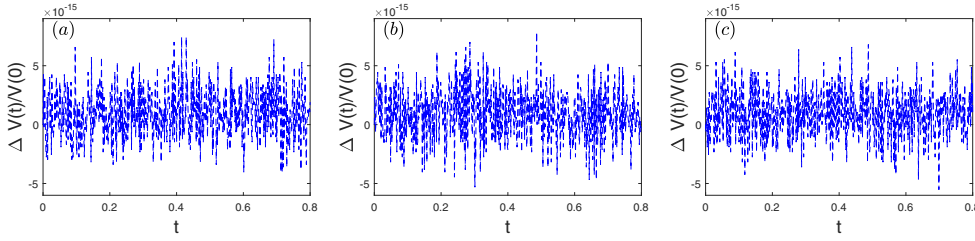


FIG. 4.1. Plot of the normalized volume change  $\frac{\Delta V(t)}{V(0)}$  for different cases: (a) for Case 1, (b) for Case 2, and (c) for Case 3.

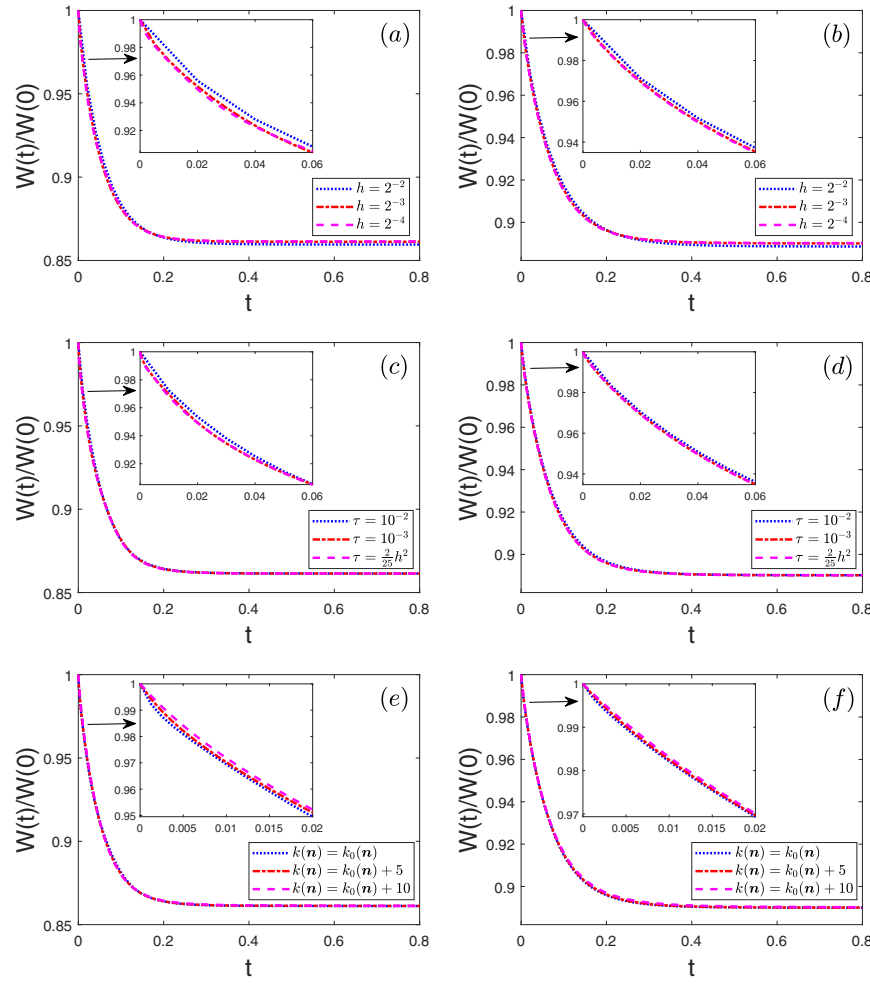


FIG. 4.2. Plot of the normalized energy  $\frac{W(t)}{W(0)}$  for weak anisotropy  $\gamma(\mathbf{n}) = 1 + \frac{1}{4}(n_1^4 + n_2^4 + n_3^4)$  (left column) and strong anisotropy  $\gamma(\mathbf{n}) = 1 + \frac{1}{2}(n_1^4 + n_2^4 + n_3^4)$  (right column) for with fixed  $k(\mathbf{n}) = k_0(\mathbf{n})$  for different  $h$  and  $\tau$  (top row with (a) and (b)) and for fixed  $h = 2^{-4}$  and different  $\tau$  (middle row with (c) and (d)), and with fixed  $h = 2^{-4}, \tau = \frac{2}{25}h^2$  for different  $k(\mathbf{n})$  (bottom row with (e) and (f)).

around  $10^{-15}$ , which is close to the machine epsilon at around  $10^{-16}$ , and thus it confirms numerically volume conservation of the SP-PFEM in Theorem 2.3. Figure 4.2

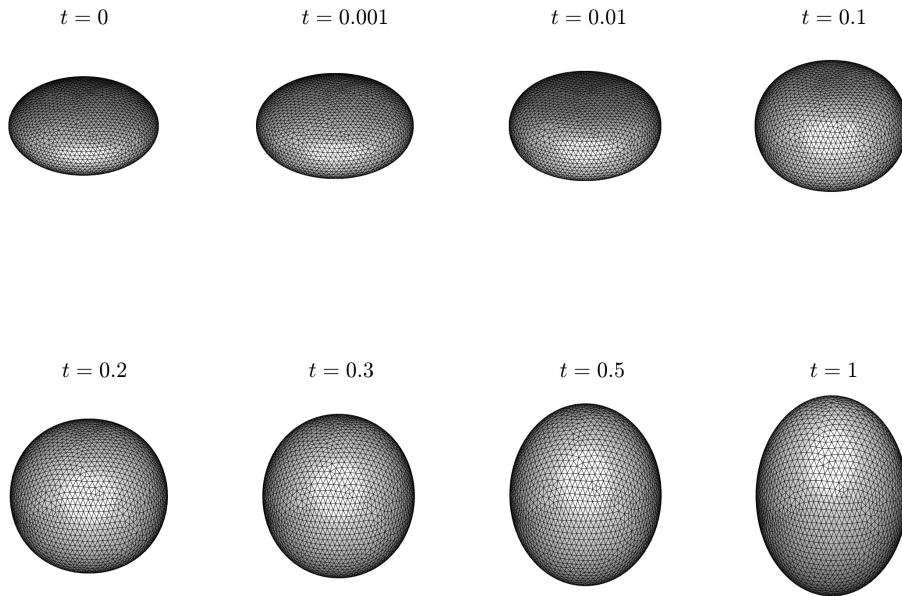


FIG. 4.3. *Evolution of a  $2 \times 2 \times 1$  ellipsoid by anisotropic surface diffusion with a weak anisotropy  $\gamma(\mathbf{n}) = \sqrt{n_1^2 + n_2^2 + 2n_3^2}$  and  $k(\mathbf{n}) = k_0(\mathbf{n})$  at different times.*

plots the normalized energy  $\frac{W(t)}{W(0)}$  for different mesh size  $h$  with  $\tau = \frac{2}{25}h^2$  and for different  $\tau$  with a fixed mesh size  $h = 2^{-4}$ . We observe that the normalized energy  $\frac{W(t)}{W(0)}$  is monotonically decreasing in time for all cases, which again confirms the unconditional energy stability of the SP-PFEM in Theorem 2.3. Furthermore, our numerical results suggest that different stabilizing functions  $k(\mathbf{n})$  do not pollute the energy too much, and thus we can choose a relatively large stabilizing function  $k(\mathbf{n})$  in practical computations.

Finally, we use the SP-PFEM (2.23) to investigate the motion by anisotropic surface diffusion with different anisotropies. We consider the weak anisotropy  $\gamma(\mathbf{n}) = \sqrt{n_1^2 + n_2^2 + 2n_3^2}$  with  $k(\mathbf{n}) = k_0(\mathbf{n})$ . The evolutions of a smooth  $2 \times 2 \times 1$  ellipsoid and a nonsmooth  $2 \times 2 \times 1$  cuboid are shown in Figures 4.3 and 4.4, respectively. We choose the mesh size  $h = 2^{-4}$  and the time step size  $\tau = \frac{2}{25}h^2$ , and the ellipsoid and the cuboid are initially approximated by 10718 triangles and 5361 vertices, and 32768 triangles and 16386 vertices, respectively. By comparing the two figures, we find the two numerical equilibria are close in shape, which indicates our SP-PFEM (2.23) is robust in capturing the equilibrium shape for different initial shapes. We can see that the meshes are well distributed during the evolution, and there is no need to remesh during the evolution.

Then we show the evolution of a strong anisotropy  $\gamma(\mathbf{n}) = 1 + \frac{1}{2}(n_1^4 + n_2^4 + n_3^4)$  from a  $2 \times 2 \times 1$  cuboid, and the parameters are chosen the same as in previous weak anisotropy. As can be seen from Figure 4.5, the large and flat facets may be broken into small facets, and the small facets may also merge into a large facet. Moreover, we note from Figure 4.5 that the triangulations become dense at the edges where the facets merge but become sparse at the other edges and at the interior of the facets where the weighted mean curvature  $\mu$  is almost a constant. This indicates the meshes achieve the same “stable fashion” as in the BGN scheme [13].

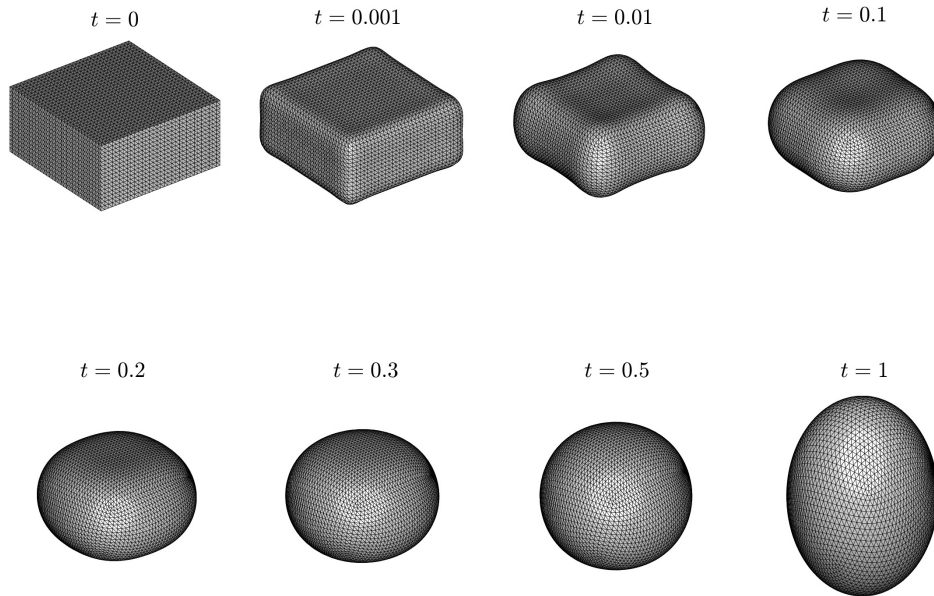


FIG. 4.4. *Evolution of a  $2 \times 2 \times 1$  cuboid by anisotropic surface diffusion with a weak anisotropy  $\gamma(\mathbf{n}) = \sqrt{n_1^2 + n_2^2 + 2n_3^2}$  and  $k(\mathbf{n}) = k_0(\mathbf{n})$  at different times.*

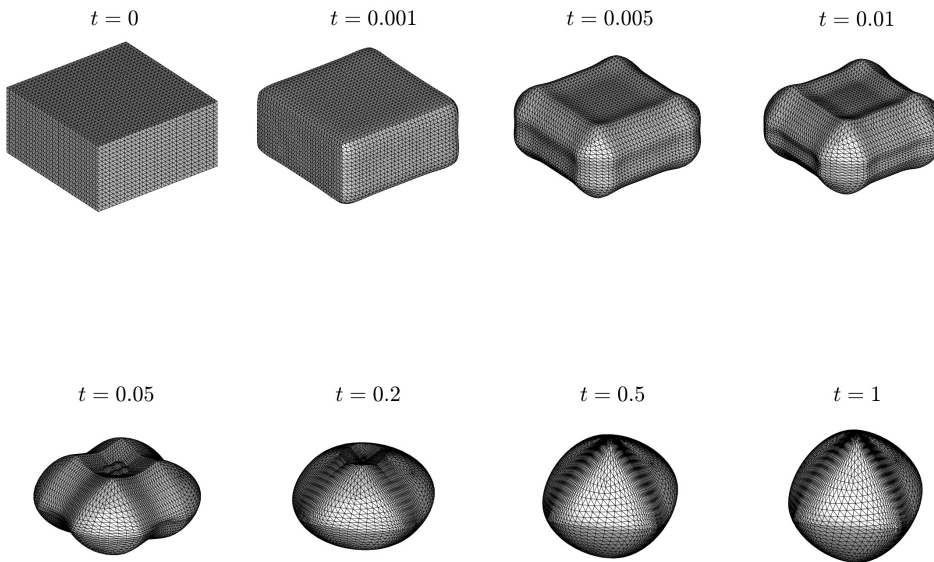


FIG. 4.5. *Evolution of a  $2 \times 2 \times 1$  cuboid by anisotropic surface diffusion with a strong anisotropy  $\gamma(\mathbf{n}) = 1 + \frac{1}{2}(n_1^4 + n_2^4 + n_3^4)$  and  $k(\mathbf{n}) = k_0(\mathbf{n})$  at different times.*

**5. Conclusions.** By generalizing the symmetrized surface energy matrix  $Z_k(\mathbf{n})$  in 2D proposed in [6] to 3D, which depends on the Cahn–Hoffman  $\xi$ -vector and a stabilizing function  $k(\mathbf{n})$ , we derived a symmetrized and conservative variational formulation for anisotropic surface diffusion with an anisotropic surface energy  $\gamma(\mathbf{n})$ . A structure-preserving parametric finite element method, or SP-PFEM, was proposed to discretize the variational problem, which preserves the volume in the fully discretized

level. Under the simple and mild condition (1.5) on  $\gamma(\mathbf{n})$  for both weak and strong surface energy anisotropy, we showed that the SP-PFEM is unconditionally energy stable when the stabilizing function  $k(\mathbf{n})$  satisfies  $k(\mathbf{n}) \geq k_0(\mathbf{n})$  with  $k_0(\mathbf{n})$  being the minimal stabilizing function. Numerical examples were presented to demonstrate the efficiency and accuracy as well as the mesh robustness of the proposed SP-PFEM for simulating anisotropic surface diffusion. Finally, we point out that the symmetrized surface energy matrix  $\mathbf{Z}_k(\mathbf{n})$  can be adapted to derive symmetrized and conservative variational formulations for other geometric flows with anisotropic surface energy  $\gamma(\mathbf{n})$ , such as the anisotropic mean curvature flow [11], the Stefan problem [14], and the anisotropic elastic flow [16].

### Appendix A. The Cahn–Hoffman $\xi$ -vectors for several anisotropic surface energies.

(i) For the ellipsoidal anisotropic surface energy [11]

$$(A.1) \quad \gamma(\mathbf{n}) = \sqrt{\mathbf{n}^T \mathbf{G} \mathbf{n}}, \quad \mathbf{n} \in \mathbb{S}^2,$$

where  $\mathbf{G} \in \mathbb{R}^{3 \times 3}$  is a symmetric positive definite matrix, we have

$$(A.2) \quad \gamma(\mathbf{p}) = \sqrt{\mathbf{p}^T \mathbf{G} \mathbf{p}} \quad \forall \mathbf{p} \in \mathbb{R}_*^3 := \mathbb{R}^3 \setminus \{\mathbf{0}\},$$

$$(A.3) \quad \boldsymbol{\xi} = \boldsymbol{\xi}(\mathbf{n}) = \gamma(\mathbf{n})^{-1} \mathbf{G} \mathbf{n} \quad \forall \mathbf{n} \in \mathbb{S}^2,$$

$$(A.4) \quad \mathbf{H}_\gamma(\mathbf{n}) = \gamma(\mathbf{n})^{-3/2} [\gamma(\mathbf{n})^2 \mathbf{G} - (\mathbf{G} \mathbf{n})(\mathbf{G} \mathbf{n})^T].$$

It is easy to check that  $\mathbf{H}_\gamma(\mathbf{n})$  is semipositive definite by using the Cauchy inequality, which indicates the ellipsoidal anisotropy is weakly anisotropic.

(ii) For the  $l^r$ -norm ( $r \geq 2$ ) metric anisotropic surface energy [6]

$$(A.5) \quad \gamma(\mathbf{n}) = (|n_1|^r + |n_2|^r + |n_3|^r)^{1/r}, \quad \mathbf{n} = (n_1, n_2, n_3)^T \in \mathbb{S}^2,$$

we have

$$(A.6) \quad \gamma(\mathbf{p}) = \|\mathbf{p}\|_{l^r} = (|p_1|^r + |p_2|^r + |p_3|^r)^{\frac{1}{r}} \quad \forall \mathbf{p} = (p_1, p_2, p_3)^T \in \mathbb{R}_*^3,$$

$$(A.7) \quad \boldsymbol{\xi} = \boldsymbol{\xi}(\mathbf{n}) = \gamma(\mathbf{n})^{1-r} \begin{pmatrix} |n_1|^{r-2} n_1 \\ |n_2|^{r-2} n_2 \\ |n_3|^{r-2} n_3 \end{pmatrix} \quad \forall \mathbf{n} = (n_1, n_2, n_3)^T \in \mathbb{S}^2,$$

$$(A.8) \quad \mathbf{H}_\gamma(\mathbf{n}) = (r-1)\gamma(\mathbf{n})^{1-2r} \begin{pmatrix} |n_1|^{r-2}(|n_2|^r + |n_3|^r) & * & * \\ -|n_1 n_2|^{r-2} n_1 n_2 & * & * \\ -|n_1 n_3|^{r-2} n_1 n_3 & * & * \end{pmatrix},$$

where the \* entries can be deduced from other entries. By checking leading principal minors, we know that  $\mathbf{H}_\gamma(\mathbf{n})$  is semipositive definite. Thus the  $l^r$ -norm anisotropy is weakly anisotropic.

(iii) For the fourfold anisotropic surface energy [24]

$$(A.9) \quad \gamma(\mathbf{n}) = 1 + \beta(n_1^4 + n_2^4 + n_3^4), \quad \mathbf{n} = (n_1, n_2, n_3)^T \in \mathbb{S}^2,$$

where  $\beta > -1$  is a given constant, we have

$$(A.10) \quad \gamma(\mathbf{p}) = (p_1^2 + p_2^2 + p_3^2)^{\frac{1}{2}} + \beta(p_1^4 + p_2^4 + p_3^4) (p_1^2 + p_2^2 + p_3^2)^{-\frac{3}{2}},$$

$$(A.11) \quad \boldsymbol{\xi} = \boldsymbol{\xi}(\mathbf{n}) = \mathbf{n} + \beta(4n_1^3 - 3n_1(n_1^4 + n_2^4 + n_3^4), *, *)^T,$$

$$(A.12) \quad \lambda_1(\mathbf{n}) + \lambda_2(\mathbf{n}) = 2(1 - 3\beta) + 36\beta(n_1^2 n_2^2 + n_2^2 n_3^2 + n_3^2 n_1^2),$$

$$(A.13) \quad \lambda_1(\mathbf{n}) \lambda_2(\mathbf{n}) = 20(n_1^4 n_2^4 + n_2^4 n_3^4 + n_3^4 n_1^4) + 72n_1^2 n_2^2 n_3^2 \geq 0.$$

Thus when  $\beta = 0$ , it is isotropic; when  $-1 < \beta < 0$  or  $0 < \beta \leq \frac{1}{3}$ , it is weakly anisotropic; and when  $\beta > \frac{1}{3}$ , it is strongly anisotropic.

(iv) Finally, for the regularized BGN anisotropic surface energy [13]

$$(A.14) \quad \gamma(\mathbf{n}) = \left( \sum_{l=1}^L (\mathbf{n}^T \mathbf{G}_l \mathbf{n})^{r/2} \right)^{1/r},$$

where  $r \geq 1$  and  $\mathbf{G}_1, \mathbf{G}_2, \dots, \mathbf{G}_L$  are symmetric positive definite matrices, we get

$$(A.15) \quad \gamma(\mathbf{p}) = \left( \sum_{l=1}^L (\mathbf{p}^T \mathbf{G}_l \mathbf{p})^{r/2} \right)^{1/r} \quad \forall \mathbf{p} \in \mathbb{R}_*^3,$$

$$(A.16) \quad \boldsymbol{\xi} = \boldsymbol{\xi}(\mathbf{n}) = \gamma(\mathbf{n})^{1-r} \sum_{l=1}^L \gamma_l^{r-2}(\mathbf{n}) \mathbf{G}_l \mathbf{n} \quad \forall \mathbf{n} \in \mathbb{S}^1,$$

$$(A.17) \quad \mathbf{H}_\gamma(\mathbf{n}) = \gamma(\mathbf{n})^{1-2r} (\mathbf{M}_1 + (r-1)\mathbf{M}_2),$$

where  $\gamma_l(\mathbf{n}) := \sqrt{\mathbf{n}^T \mathbf{G}_l \mathbf{n}}$  for  $l = 1, 2, \dots, L$ , and

$$\begin{aligned} \mathbf{M}_1 &= \gamma(\mathbf{n})^r \sum_{l=1}^L \gamma_l(\mathbf{n})^{r-4} (\gamma_l(\mathbf{n})^2 \mathbf{G}_l - (\mathbf{G}_l \mathbf{n})(\mathbf{G}_l \mathbf{n})^T), \\ \mathbf{M}_2 &= \gamma(\mathbf{n})^r \sum_{l=1}^L (\mathbf{G}_l \mathbf{n})(\mathbf{G}_l \mathbf{n})^T \gamma_l^{r-4}(\mathbf{n}) - \left( \sum_{l=1}^L \gamma_l^{r-2}(\mathbf{n}) \mathbf{G}_l \mathbf{n} \right) \left( \sum_{l=1}^L \gamma_l^{r-2}(\mathbf{n}) \mathbf{G}_l \mathbf{n} \right)^T. \end{aligned}$$

By the Cauchy inequality, we obtain that  $\mathbf{M}_1$  and  $\mathbf{M}_2$  are semipositive definite. Thus the BGN anisotropy is weakly anisotropic when  $r \geq 1$ .

## REFERENCES

- [1] L. ARMELAO, D. BARRECA, G. BOTTARO, A. GASPAROTTO, S. GROSS, C. MARAGNO, AND E. TONDELLO, *Recent trends on nanocomposites based on Cu, Ag and Au clusters: A closer look*, Coord. Chem. Rev., 250 (2006), pp. 1294–1314.
- [2] R. ASARO AND W. TILLER, *Interface morphology development during stress corrosion cracking: Part I. Via surface diffusion*, Metall. Mater. Trans. B, 3 (1972), pp. 1789–1796.
- [3] E. BÄNSCH, P. MORIN, AND R. H. NOCHETTO, *Surface diffusion of graphs: Variational formulation, error analysis, and simulation*, SIAM J. Numer. Anal., 42 (2004), pp. 773–799.
- [4] W. BAO, H. GARCKE, R. NÜRNBERG, AND Q. ZHAO, *Volume-preserving parametric finite element methods for axisymmetric geometric evolution equations*, J. Comput. Phys., 460 (2022), 111180.
- [5] W. BAO, H. GARCKE, R. NÜRNBERG, AND Q. ZHAO, *A structure-preserving finite element approximation of surface diffusion for curve networks and surface clusters*, Numer. Methods Partial Differential Equation, 39 (2023), pp. 759–794.
- [6] W. BAO, W. JIANG, AND Y. LI, *A symmetrized parametric finite element method for anisotropic surface diffusion of closed curves*, SIAM J. Numer. Anal., 61 (2023), pp. 617–641.
- [7] W. BAO, W. JIANG, Y. WANG, AND Q. ZHAO, *A parametric finite element method for solid-state dewetting problems with anisotropic surface energies*, J. Comput. Phys., 330 (2017), pp. 380–400.
- [8] W. BAO AND Q. ZHAO, *An energy-stable parametric finite element method for simulating solid-state dewetting problems in three dimensions*, J. Comput. Math., to appear.
- [9] W. BAO AND Q. ZHAO, *A structure-preserving parametric finite element method for surface diffusion*, SIAM J. Numer. Anal., 59 (2021), pp. 2775–2799.
- [10] J. W. BARRETT, H. GARCKE, AND R. NÜRNBERG, *A parametric finite element method for fourth order geometric evolution equations*, J. Comput. Phys., 222 (2007), pp. 441–467.
- [11] J. W. BARRETT, H. GARCKE, AND R. NÜRNBERG, *Numerical approximation of anisotropic geometric evolution equations in the plane*, IMA J. Numer. Anal., 28 (2008), pp. 292–330.

- [12] J. W. BARRETT, H. GARCKE, AND R. NÜRNBERG, *On the parametric finite element approximation of evolving hypersurfaces in  $\mathbb{R}^3$* , J. Comput. Phys., 227 (2008), pp. 4281–4307.
- [13] J. W. BARRETT, H. GARCKE, AND R. NÜRNBERG, *A variational formulation of anisotropic geometric evolution equations in higher dimensions*, Numer. Math., 109 (2008), pp. 1–44.
- [14] J. W. BARRETT, H. GARCKE, AND R. NÜRNBERG, *On stable parametric finite element methods for the stefan problem and the Mullins–Sekerka problem with applications to dendritic growth*, J. Comput. Phys., 229 (2010), pp. 6270–6299.
- [15] J. W. BARRETT, H. GARCKE, AND R. NÜRNBERG, *Numerical computations of faceted pattern formation in snow crystal growth*, Phys. Rev. E, 86 (2012), 011604.
- [16] J. W. BARRETT, H. GARCKE, AND R. NÜRNBERG, *Parametric approximation of isotropic and anisotropic elastic flow for closed and open curves*, Numer. Math., 120 (2012), pp. 489–542.
- [17] J. W. BARRETT, H. GARCKE, AND R. NÜRNBERG, *Parametric finite element approximations of curvature-driven interface evolutions*, in Geometric Partial Differential Equations—Part I, Handb. Numer. Anal. 21, Elsevier, Amsterdam, 2020, pp. 275–423.
- [18] O. BEKHTEREVA, Y. GAVRILYUK, V. LIFSHITS, AND B. CHURUSOV, *Indium surface phase formation on Si (111) surface and their role in diffusion and desorption*, poverkhnost, Physika Khimiia i Mekhanika, 8 (1988), p. 54.
- [19] J. CAHN AND D. HOFFMAN, *A vector thermodynamics for anisotropic surfaces: I. Curved and faceted surfaces*, in The Selected Works of John W. Cahn, Wiley, New York, 1998, pp. 315–324.
- [20] J. W. CAHN AND J. E. TAYLOR, *Overview no. 113 surface motion by surface diffusion*, Acta Metall. Mater., 42 (1994), pp. 1045–1063.
- [21] L.-S. CHANG, E. RABKIN, B. STRAUMAL, B. BARETZKY, AND W. GUST, *Thermodynamic aspects of the grain boundary segregation in Cu (Bi) alloys*, Acta Mater., 47 (1999), pp. 4041–4046.
- [22] U. CLARENZ, U. DIEWALD, AND M. RUMPF, *Anisotropic geometric diffusion in surface processing*, in IEEE Proceedings of Visualitzion, 2000.
- [23] K. DECKELNICK AND G. DZIUK, *A fully discrete numerical scheme for weighted mean curvature flow*, Numer. Math., 91 (2002), pp. 423–452.
- [24] K. DECKELNICK, G. DZIUK, AND C. M. ELLIOTT, *Computation of geometric partial differential equations and mean curvature flow*, Acta Numer., 14 (2005), pp. 139–232.
- [25] P. DU, M. KHENNER, AND H. WONG, *A tangent-plane marker-particle method for the computation of three-dimensional solid surfaces evolving by surface diffusion on a substrate*, J. Comput. Phys., 229 (2010), pp. 813–827.
- [26] I. FONSECA, A. PRATELLI, AND B. ZWICKNAGL, *Shapes of epitaxially grown quantum dots*, Arch. Ration. Mech. Anal., 214 (2014), pp. 359–401.
- [27] Y. GIGA, *Surface Evolution Equations*, Springer, New York, 2006.
- [28] M. E. GURTIN AND M. E. JABBOUR, *Interface evolution in three dimensions with curvature-dependent energy and surface diffusion: Interface-controlled evolution, phase transitions, epitaxial growth of elastic films*, Arch. Ration. Mech. Anal., 163 (2002), pp. 171–208.
- [29] K. HAUFFE, *The application of the theory of semiconductors to problems of heterogeneous catalysis*, in Advances in Catalysis and Related Subjects, Adv. Catal. 7, Elsevier, Amsterdam, 1955, pp. 213–257.
- [30] F. HAUSER AND A. VOIGT, *A discrete scheme for parametric anisotropic surface diffusion*, J. Sci. Comput., 30 (2007), pp. 223–235.
- [31] D. W. HOFFMAN AND J. W. CAHN, *A vector thermodynamics for anisotropic surfaces: I. Fundamentals and application to plane surface junctions*, Surf. Sci., 31 (1972), pp. 368–388.
- [32] W. JIANG, W. BAO, C. V. THOMPSON, AND D. J. SROLOVITZ, *Phase field approach for simulating solid-state dewetting problems*, Acta Mater., 60 (2012), pp. 5578–5592.
- [33] W. JIANG, Y. WANG, Q. ZHAO, D. J. SROLOVITZ, AND W. BAO, *Solid-state dewetting and island morphologies in strongly anisotropic materials*, Scr. Mater., 115 (2016), pp. 123–127.
- [34] W. JIANG AND Q. ZHAO, *Sharp-interface approach for simulating solid-state dewetting in two dimensions: A Cahn–Hoffman  $\xi$ -vector formulation*, Phys. D, 390 (2019), pp. 69–83.
- [35] Y. LI AND W. BAO, *An energy-stable parametric finite element method for anisotropic surface diffusion*, J. Comput. Phys., 446 (2021), 110658.
- [36] Z. LI, H. ZHAO, AND H. GAO, *A numerical study of electro-migration voiding by evolving level set functions on a fixed cartesian grid*, J. Comput. Phys., 152 (1999), pp. 281–304.
- [37] W. W. MULLINS, *Theory of thermal grooving*, J. Appl. Phys., 28 (1957), pp. 333–339.

- [38] M. NAFFOUTI, R. BACKOFEN, M. SALVALAGLIO, T. BOTTEIN, M. LODARI, A. VOIGT, T. DAVID, A. BENKOUDIER, I. FRAJ, L. FAVRE, A. RONDA, I. BERBEZIER, D. GROSSO, M. ABBARCHI, AND M. BOLLANI, *Complex dewetting scenarios of ultrathin silicon films for large-scale nanoarchitectures*, Sci. Adv., 3 (2017), 1472.
- [39] P. POZZI, *Anisotropic mean curvature flow for two-dimensional surfaces in higher codimension: A numerical scheme*, Interfaces Free Bound., 10 (2008), pp. 539–576.
- [40] P. SIMULATION, *CFDTool - MATLAB CFD Simulation GUI & Toolbox*, 2022, <https://github.com/precise-simulation/cfdtool/releases/tag/1.9.2>.
- [41] J. E. TAYLOR, *Mean curvature and weighted mean curvature*, Acta Metall. Mater., 40 (1992), pp. 1475–1485.
- [42] J. E. TAYLOR AND J. W. CAHN, *Linking anisotropic sharp and diffuse surface motion laws via gradient flows*, J. Stat. Phys., 77 (1994), pp. 183–197.
- [43] J. E. TAYLOR, J. W. CAHN, AND C. A. HANDWERKER, *Overview no. 98. I—Geometric models of crystal growth*, Acta Metal. Mater., 40 (1992), pp. 1443–1474.
- [44] C. V. THOMPSON, *Solid-state dewetting of thin films*, Annu. Rev. Mater. Res., 42 (2012), pp. 399–434.
- [45] Y. WANG, W. JIANG, W. BAO, AND D. J. SROLOVITZ, *Sharp interface model for solid-state dewetting problems with weakly anisotropic surface energies*, Phys. Rev. B, 91 (2015), 045303.
- [46] A. WHEELER, *Cahn-Hoffman  $\xi$ -vector and its relation to diffuse interface models of phase transitions*, J. Stat. Phys., 95 (1999), pp. 1245–1280.
- [47] L. XIA, A. F. BOWER, Z. SUO, AND C. SHIH, *A finite element analysis of the motion and evolution of voids due to strain and electromigration induced surface diffusion*, J. Mech. Phys. Solids, 45 (1997), pp. 1473–1493.
- [48] Y. XU AND C.-W. SHU, *Local discontinuous Galerkin method for surface diffusion and Willmore flow of graphs*, J. Sci. Comput., 40 (2009), pp. 375–390.
- [49] J. YE AND C. V. THOMPSON, *Mechanisms of complex morphological evolution during solid-state dewetting of single-crystal nickel thin films*, Appl. Phys. Lett., 97 (2010), 071904.
- [50] Q. ZHAO, W. JIANG, AND W. BAO, *A parametric finite element method for solid-state dewetting problems in three dimensions*, SIAM J. Sci. Comput., 42 (2020), pp. B327–B352.